

# Uncertainty Estimation and Quantification for LLMs: A Simple Supervised Approach

Linyu Liu<sup>†,§,\*</sup> Yu Pan<sup>‡,\*</sup> Xiaocheng Li<sup>◊</sup> Guanting Chen<sup>†</sup>

<sup>†</sup>University of North Carolina <sup>§</sup>Tsinghua University <sup>‡</sup>HKUST(GZ) <sup>◊</sup>Imperial College London

## Abstract

In this paper, we study the problem of uncertainty estimation and calibration for LLMs. We first formulate the uncertainty estimation problem for LLMs and then propose a supervised approach that takes advantage of the labeled datasets and estimates the uncertainty of the LLMs' responses. Based on the formulation, we illustrate the difference between the uncertainty estimation for LLMs and that for standard ML models and explain why the hidden neurons of the LLMs may contain uncertainty information. Our designed approach demonstrates the benefits of utilizing hidden activations to enhance uncertainty estimation across various tasks and shows robust transferability in out-of-distribution settings. We distinguish the uncertainty estimation task from the uncertainty calibration task and show that a better uncertainty estimation mode leads to a better calibration performance. Furthermore, our method is easy to implement and adaptable to different levels of model accessibility including black box, grey box, and white box.

## 1 Introduction

Large language models (LLMs) have marked a significant milestone in the advancement of natural language processing (Radford et al., 2019; Brown et al., 2020; Ouyang et al., 2022; Bubeck et al., 2023), showcasing remarkable capabilities in understanding and generating human-like text. However, one pressing issue for the LLMs is their propensity to hallucinate (Rawte et al., 2023) and generate misleading or entirely fabricated information that can significantly undermine their trustworthiness and reliability. The task of uncertainty estimation has then emerged to be an important problem that aims to determine the confidence levels of LLMs' outputs. While the problem of uncertainty estimation and calibration has seen considerable development within the general machine learning and deep learning domains (Abdar et al., 2021; Gawlikowski et al., 2023), we see less development in the domain of LLMs. One of the major challenges is the difference in the format of the output: while machine learning and deep learning typically involve fixed-dimensional outputs, natural language generation (NLG) tasks central to LLM applications require handling variable outputs that carry semantic meanings.

Existing uncertainty estimation approaches for LLMs usually involve designing uncertainty metrics for their outputs. For black-box LLMs, these metrics are computed by examining aspects like the generated outputs' consistency, similarity, entropy, and other relevant characteristics (Lin et al., 2023; Manakul et al., 2023; Kuhn et al., 2023; Hou et al., 2023; Farquhar et al., 2024). Given the complexity of LLMs' underlying architectures, semantic information may be diluted when processing through self-attention mechanisms and during token encoding/decoding. To address this issue, a growing stream of literature argues that hidden layers' activation values within the LLMs offer insights into the LLMs' knowledge and confidence (Slobodkin et al., 2023; Ahdritz et al., 2024; Duan et al., 2024). Based on this argument,

---

\*Equal contribution.

white-box LLMs, which allow access to more of LLMs’ inner values, such as logits and hidden layers, are believed to have the capacity to offer a more nuanced understanding and improved uncertainty estimation results (Verma et al., 2023; Chen et al., 2024; Plaut et al., 2024).

Most state-of-the-art uncertainty estimation methods in NLG-related tasks are developed in an unsupervised manner (Lin et al., 2022; Kuhn et al., 2023; Chen et al., 2024; Farquhar et al., 2024). However, in the realm of LLMs, there is increasing evidence suggesting the benefits of pursuing supervised approaches. For instance, LLMs’ outputs and their internal states can offer conflicting information about truthfulness (Liu et al., 2023), and determining whether outputs or internal states are more reliable sources of information often varies from one scenario to another. This phenomenon underscores the potential advantages of a supervised learning approach, which can adaptively leverage both types of information for better uncertainty estimation. Meanwhile, employing a supervised learning approach to utilize hidden information within LLMs for uncertainty estimation remains relatively uncharted territory. Prior to the advent of LLM, a line of literature has studied incorporating supervised learning approaches for uncertainty estimation and calibration (Desai and Durrett, 2020) for white-box (Zhang et al., 2021) and black-box (Ye and Durrett, 2021) natural language processing (NLP) models. However, the LLMs distinguish themselves from earlier NLP models through their architectures, training methodologies, and the datasets used. Consequently, there is a need to study and investigate supervised uncertainty estimation approaches specifically tailored for LLMs. There is also a recently expanding body of literature that employs supervised approaches that leverage hidden layers’ information for hallucination detection within LLMs (CH-Wang et al., 2023; Azaria and Mitchell, 2023; Ahdritz et al., 2024). However, there is not so much of a consensus on the definition of hallucination while the uncertainty estimation problem is more well defined. Consequently, questions regarding the practicality, effectiveness, and potential of these supervised approaches to improve uncertainty estimation practices in LLM remain unanswered.

Our contributions are three-fold:

- First, we formulate the problem of uncertainty estimation for LLMs. We explore the nuanced distinctions between uncertainty estimation and calibration for LLMs, and theoretically demonstrate how uncertainty estimation for LLMs differs from that in traditional ML models.
- Second, motivated by the above findings, we propose a supervised method for the uncertainty estimation problem. Specifically, the method aims to train an uncertainty estimation function that maps the hidden activations of the LLMs, and the probability-related information of the LLMs (when generating the response) to an uncertainty score that captures the LLM’s confidence about its response. This supervised approach is systematically designed for straightforward implementation and broad applicability, suitable for black-box, grey-box, and white-box LLMs.
- Third, we conduct numerical experiments on NLP tasks including question answering, machine translation, and multiple choice to evaluate our proposed approach against existing benchmarks. We systematically investigate the working mechanism of uncertainty quantification.

## 1.1 Related literature

**Uncertainty estimation for natural language generalization.** The uncertainty estimation and calibration for traditional machine learning is relatively well-studied (Abdar et al., 2021; Gawlikowski et al., 2023). However, with the rapid development of LLMs, there is a pressing need to better understand the uncertainty for LLMs’ responses, and measuring the uncertainty from sentences instead of a fixed-dimension output is more challenging. One stream of work has been focusing on unsupervised methods that leverage entropy (Malinin and Gales, 2021), similarity (Fomicheva et al., 2020; Lin et al., 2022), semantic (Kuhn et al., 2023; Duan et al., 2023; Farquhar et al., 2024), logit or hidden states’ information (Kadavath et al., 2022; Chen et al., 2024; Su et al., 2024; Plaut et al., 2024) to craft a uncertainty metric

that helps to quantify uncertainty. For black-box models, some of the metrics can be computed based on multiple sampled output of the LLMs (Malinin and Gales, 2021; Lin et al., 2023; Manakul et al., 2023); while for white-box models, more information such as the output’s distribution, the value of the logit and hidden layers make computing the uncertainty metric easier. We also refer to Desai and Durrett (2020); Zhang et al. (2021); Ye and Durrett (2021); Si et al. (2022); Quach et al. (2023); Kumar et al. (2023); Mohri and Hashimoto (2024) for other related uncertainty estimation methods such as calibration and conformal prediction.

**Hallucination detection.** Recently, there is a trend of adopting uncertainty estimation approaches for hallucination detection. The rationale is that the information of the value of logits and the hidden states contain some of the LLMs’ beliefs about the trustworthiness of its generated output. By taking the activations of hidden layers as input, Azaria and Mitchell (2023) train a classifier to predict hallucinations, and Verma et al. (2023) develop epistemic neural networks aimed at reducing hallucinations. Slobodkin et al. (2023) demonstrate that the information from hidden layers of LLMs’ output can indicate the answerability of an input query, providing indirect insights into hallucination occurrences. Chen et al. (2024) develop an unsupervised metric that leverages the internal states of LLMs to perform hallucination detection. More related works on hallucination detection can be found in CH-Wang et al. (2023); Duan et al. (2024); Xu et al. (2024). While there is a lack of a rigorous definition of hallucination, and its definition varies in the above-mentioned literature, the uncertainty estimation problem can be well defined, and our results on uncertainty estimation can also help the task of hallucination detection.

**Leveraging LLMs’ hidden activation.** The exploration of hidden states within LLMs has been studied to better understand LLMs’ behavior. Mielke et al. (2022) leverage the language model’s hidden states to train a calibrator that predicts the likelihood of outputs’ correctness. With an unsupervised approach, Burns et al. (2022) utilizes hidden activations in language models to represent knowledge about the trustfulness of their outputs. Liu et al. (2023) show that LLMs’ outputs and their internal states can offer conflicting information about truthfulness, and determining whether outputs or internal states are more reliable sources of information often varies from one scenario to another. By taking the activations of hidden layers as input, Ahdriz et al. (2024) employ a linear probe to show that hidden layers’ information from LLMs can be used to differentiate between epistemic and aleatoric uncertainty. Duan et al. (2024) experimentally reveal the variations in hidden layers’ activations when LLMs generate true versus false responses. Lastly, Li et al. (2024) enhance the truthfulness of LLMs during inference time by adjusting the hidden activations’ values in specific directions.

We also remark on the following two aspects:

- **Fine-tuning:** For all the numerical experiments in this paper, we do not perform any fine-tuning with respect to the underlying LLMs. While the fine-tuning procedure generally boosts the LLMs’ performance on a downstream task, our methods can still be applied for a fine-tuned LLM, which we leave as future work.
- **Hallucination:** The hallucination problem has been widely studied in the LLM literature. Yet, as mentioned earlier, it seems there is no consensus on a rigorous definition of what hallucination refers to in the context of LLMs. For example, when an image classifier wrongly classifies a cat image as a dog, we do not say the image classifier hallucinates, then why or when we should say the LLMs hallucinate when they make a mistake? Comparatively, the uncertainty estimation problem is more well-defined, and we provide a mathematical formulation for the uncertainty estimation task for LLMs. Also, we believe our results on uncertainty estimation can also help with a better understanding of the hallucination phenomenon and tasks such as hallucination detection.

## 2 Problem Setup

Consider the following environment where one interacts with LLMs through prompts and responses: An LLM is given with an input prompt  $\mathbf{x} = (x_1, x_2, \dots, x_k) \in \mathcal{X}$  with  $x_i \in \mathcal{V}$  representing the  $i$ -th token of the prompt. Here  $\mathcal{V}$  denotes the vocabulary for all the tokens. Then the LLM generates its response  $\mathbf{y} = (y_1, y_2, \dots, y_m) \in \mathcal{Y}$  (randomly) following the probability distribution

$$y_j \sim p_\theta(\cdot | \mathbf{x}, y_1, y_2, \dots, y_{j-1}).$$

Here the probability distribution  $p_\theta$  denotes the distribution (over vocabulary  $\mathcal{V}$ ) as the LLM’s output, and  $\theta$  encapsulates all the parameters of the LLM. The conditional part includes the prompt  $\mathbf{x}$  and all the tokens  $y_1, y_2, \dots, y_{j-1}$  generated preceding the current position.

We consider using the LLM for some downstream NLP tasks such as question answering, multiple choice, and machine translation. Such a task usually comes with an evaluation/scoring function that evaluates the quality of the generated response  $s(\cdot, \cdot) : \mathcal{Y} \times \mathcal{Y} \rightarrow [0, 1]$ . For each pair of  $(\mathbf{x}, \mathbf{y})$ , the evaluation function rates the response  $\mathbf{y}$  with the score  $z := s(\mathbf{y}_{\text{true}}, \mathbf{y})$  where  $\mathbf{y}_{\text{true}}$  is the true response for the prompt  $\mathbf{x}$ . The true response  $\mathbf{y}_{\text{true}}$  is usually decided by factual truth, humans, or domain experts. It does not hurt to assume a larger score represents a better answer;  $z = 1$  indicates a perfect answer, while  $z = 0$  says the response  $\mathbf{y}$  is off the target.

We define the task of *uncertainty estimation* for LLMs as the learning of a function  $g$  that predicts the score

$$g(\mathbf{x}, \mathbf{y}) \approx \mathbb{E}[s(\mathbf{y}, \mathbf{y}_{\text{true}}) | \mathbf{x}, \mathbf{y}] \quad (1)$$

where the expectation on the right-hand side is taken with respect to the (possible) randomness of the true response  $\mathbf{y}_{\text{true}}$ . We emphasize two points on this task definition: The uncertainty function  $g$  takes the prompt  $\mathbf{x}$  and  $\mathbf{y}$  as its inputs. This implies (i) the true and predicted uncertainty score can and should depend on the specific realization of the response  $\mathbf{y}$  and (ii) the uncertainty function  $g$  does not require the true response  $\mathbf{y}_{\text{true}}$  as the input.

The uncertainty score function  $g$ , in the language of uncertainty calibration of ML models (Guo et al., 2017; Abdar et al., 2021), is defined in an individual (conditional) sense. That is, the predicted score  $g(\mathbf{x}, \mathbf{y})$  is hopefully precise and matches the true score on an individual level (for each prompt-response pair) but not on the population level (for a distribution of prompt-response pairs).

## 3 Uncertainty Estimation via Supervised Calibration

### 3.1 Supervised calibration

We consider a supervised approach of learning the uncertainty function  $g : \mathcal{X} \times \mathcal{Y} \rightarrow [0, 1]$ , which is similar to the standard setting of uncertainty quantification for ML/deep learning models. First, we start with a dataset of  $n$  samples

$$\mathcal{D}_{\text{raw}} = \{(\mathbf{x}_i, \mathbf{y}_i, \mathbf{y}_{i,\text{true}}, s(\mathbf{y}_i, \mathbf{y}_{i,\text{true}}))\}_{i=1}^n.$$

$\mathcal{D}_{\text{raw}}$  can be generated based on a labeled dataset for the tasks we consider. Here  $\mathbf{x}_i = (x_{i,1}, \dots, x_{i,k_i})$  and  $\mathbf{y}_i = (y_{i,1}, \dots, y_{i,m_i})$  denote the prompt and the corresponding LLM’s response, respectively.  $\mathbf{y}_{i,\text{true}}$  denotes the true response (that comes from the labeled dataset) of  $\mathbf{x}_i$ , and  $s(\mathbf{y}_i, \mathbf{y}_{i,\text{true}})$  assigns a score for the response  $\mathbf{y}_i$  based on the true answer  $\mathbf{y}_{i,\text{true}}$ .

The next is to formulate a supervised learning task based on  $\mathcal{D}_{\text{raw}}$ . Specifically, we construct

$$\mathcal{D}_{\text{un}} = \{(\mathbf{v}_i, z_i)\}_{i=1}^n$$

where  $z_i := s(\mathbf{y}_i, \mathbf{y}_{i,\text{true}}) \in [0, 1]$  denotes the target score to be predicted. The vector  $\mathbf{v}_i$  summarizes useful features for the  $i$ -th sample based on  $(\mathbf{x}_i, \mathbf{y}_i)$ . That is, a supervised learning task on the dataset  $\mathcal{D}_{\text{un}}$  coincides exactly to the definition of the uncertainty estimation task in (1). We mainly consider features from two sources when constructing  $\mathbf{v}_i$  based on  $(\mathbf{x}_i, \mathbf{y}_i)$ :

*White-box features:* LLM’s hidden-layer activations. We feed  $(\mathbf{x}_i, \mathbf{y}_i)$  as input into a LLM, and extract the corresponding hidden layers’ activations of the LLM.

*Grey-box features:* Entropy- or probability-related outputs. The entropy of a discrete distribution  $p$  over the vocabulary  $\mathcal{V}$  is defined by  $H(p) := -\sum_{v \in \mathcal{V}} p(v) \log(p(v))$ . For a prompt-response pair  $(\mathbf{x}, \mathbf{y}) = (x_1, \dots, x_k, y_1, \dots, y_m)$ , we consider as the features the entropy at each token such as  $H(p_\theta(\cdot|x_1, \dots, x_{j-1}))$  and  $H(p_\theta(\cdot|x, y_1, \dots, y_{j-1}))$  where  $p_\theta$  denotes the LLM. We defer more discussions on feature construction to Appendix C. There can be other useful features such as to ask the LLM “how certain it is about the response” (Tian et al., 2023). We do not try to exhaust all the possibility, and the aim of our paper is more about formulating the uncertainty estimation for the LLMs as a supervised task and understanding how the internal states of the LLM encode uncertainty. To the best of our knowledge, our paper is the first one to do so. Specifically, the above formulation aims for the following two outcomes: (i) an uncertainty model  $\hat{g}(\mathbf{v}_i)$  that predicts  $z_i$  and (ii) knowing whether the hidden layers carry the uncertainty information.

### 3.2 Uncertainty estimation v.s. uncertainty calibration

So far in this paper, we focus on the uncertainty estimation task which aims to predict whether the LLM makes mistakes in its response or not. There is a different but related task known as the uncertainty calibration problem. In comparison, the uncertainty calibration aims to ensure that the output from the uncertainty estimation model such as  $\hat{g}$  in above conveys a probabilistic meaning. In this sense, our paper is more focused on addressing the predictability of the LLM’s uncertainty, and we find that our supervised formulation and the LLM’s hidden activations are helpful in such a prediction task. In terms of the uncertainty calibration aspect, our developed uncertainty estimation model is compatible with all the recalibration methods for ML models in the literature of uncertainty calibration. And intuitively, a better uncertainty estimation/prediction will lead to a better-calibrated uncertainty model, which is also verified in our numerical experiments in Appendix B.

### 3.3 Why hidden layers as features?

In this subsection, we provide a simple theoretical explanation for why the hidden activations of the LLM can be useful in uncertainty estimation. Consider a binary classification task where the features  $\mathbf{X} \in \mathbb{R}^d$  and the label  $Y \in \{0, 1\}$  are drawn from a distribution  $\mathcal{P}$ . We aim to learn a model  $f : \mathbb{R}^d \rightarrow [0, 1]$  that predicts the label  $Y$  from the feature vector  $\mathbf{X}$ , and the learning of the model employs a loss function  $l(\cdot, \cdot) : [0, 1] \times [0, 1] \rightarrow \mathbb{R}$ .

**Proposition 3.1.** *Let  $\mathcal{F}$  be the class of measurable function that maps from  $\mathbb{R}^d$  to  $[0, 1]$ . Under the cross-entropy loss  $l(y, \hat{y}) = y \log(\hat{y}) + (1 - y) \log(1 - \hat{y})$ , the function  $f^*$  that minimizes the loss*

$$f^* = \arg \min_{f \in \mathcal{F}} \mathbb{E}[l(Y, f(\mathbf{X}))]$$

*is the Bayes optimal classifier*

$$f^*(\mathbf{x}) = \mathbb{P}(Y = 1 | \mathbf{X} = \mathbf{x})$$

where the expectation and the probability are taken with respect to  $(\mathbf{X}, Y) \sim \mathcal{P}$ . Moreover, the following conditional independence holds

$$Y \perp \mathbf{X} \mid f^*(\mathbf{X}).$$

The proposition is not technical and it can be easily proved by using the structure of  $f^*(\mathbf{X})$ . It states a nice (probably well-known) property of the cross-entropy loss. Specifically, the function learned under the cross-entropy loss coincides with the Bayes optimal classifier. Note that this is contingent on two requirements. First, the function class  $\mathcal{F}$  is the measurable function class. Second, it requires the function  $f^*$  learned through the population loss rather than the empirical loss/risk consisting of the training samples. The proposition also states one step further on conditional independence  $Y \perp \mathbf{X} \mid f^*(\mathbf{X})$ . This means all the information related to the label  $Y$  that is contained in  $\mathbf{X}$  is summarized in the prediction function  $f^*$ . While the numeric situation cannot be captured by such a simple theory (due to these two requirements), it provides insights into why the existing uncertainty quantification/calibration/recalibration methods do not utilize much of the original feature  $\mathbf{X}$  or the hidden-layer activations. Specifically, when a prediction model  $\hat{f} : \mathbb{R}^d \rightarrow [0, 1]$  is well-trained, the predicted score  $\hat{f}(\mathbf{X})$  should capture all the information about the true label  $Y$  contained in the features  $\mathbf{X}$ , and there is no need to get the features  $\mathbf{X}$  re-involved in the recalibration procedure. This indeed explains why the classic uncertainty quantification and calibration methods only work with the predicted score  $\hat{f}(\mathbf{X})$  for re-calibration, including Platt scaling (Platt et al., 1999), isotonic regression (Zadrozny and Elkan, 2002), temperature scaling (Guo et al., 2017), etc.

When it comes to LLMs, we will no longer have conditional independence, and that requires additional procedures to retrieve more information on  $Y$ . The following corollary states that when the underlying loss function  $\tilde{l}$  does not possess this nice property (the Bayes classifier minimizes the loss point-wise) of the cross-entropy loss, the conditional independence will collapse.

**Corollary 3.2.** *Suppose the loss function  $\tilde{l}$  satisfies*

$$\mathbb{P} \left( f^*(\mathbf{x}) \neq \arg \min_{\tilde{y} \in [0,1]} \mathbb{E} [\tilde{l}(Y, \tilde{y}) | \mathbf{X} = \mathbf{x}] \right) > 0,$$

where  $f^*$  is defined as Proposition 3.1, then for the function

$$\tilde{f} = \arg \min_{f \in \mathcal{F}} \mathbb{E} [\tilde{l}(Y, f(\mathbf{X}))],$$

where the expectation is with respect to  $(\mathbf{X}, Y) \sim \mathcal{P}$ , there exists a distribution  $\mathcal{P}$  such that the conditional independence no longer holds

$$Y \not\perp \mathbf{X} \mid \tilde{f}(\mathbf{X}).$$

Proposition 3.1 and Corollary 3.2 together illustrate the difference between uncertainty estimation for a traditional ML model and that for LLMs. For the traditional ML models, the cross-entropy loss which is commonly used for training the model is aligned toward the uncertainty calibration objective. When it comes to uncertainty estimation for LLMs, the label  $Y$  can be viewed as the binary variable for whether the LLM’s response is correct, and the features  $\mathbf{X}$  represent some features extracted from the prompt-response pair. Meanwhile, the LLMs are often pretrained with some other loss functions (for example, the negative log-likelihood loss for next-token prediction), and this causes a misalignment between the model pre-training and the uncertainty quantification task. Consequently, the original features, the prompt-response pair, may and should (in theory) contain information about the uncertainty score  $Y$  that cannot be fully captured by  $\tilde{f}(\mathbf{X})$ . This justifies why we formulate the uncertainty estimation task as

the previous subsection and take the hidden-layer activations as features to predict the uncertainty score; it also explains why we do not see much similar treatment in the mainstream uncertainty quantification literature.

### 3.4 Three regimes of supervised uncertainty estimation

In Section 3.1, we present the method of supervised uncertainty estimation under the assumption that we know the parameters of the LLMs including both the hidden activation and the output probabilities. Now we categorize the application of our method into three regimes to solve the case where the LLM is black-box and we do not have access to the parameter information.

A natural implementation of our supervised learning approach involves using an LLM to generate the response  $\mathbf{y}$  for input  $\mathbf{x}$ , and extracting insights on confidence from the same LLM’s hidden layers’ activations. This method functions effectively with white-box LLMs where hidden activations are accessible. Note that obtaining hidden layers’ activations merely requires an LLM and the prompt-response pair  $(\mathbf{x}, \mathbf{y})$ . Therefore, it is not mandatory for  $(\mathbf{x}, \mathbf{y})$  to be generated by the LLM that provides the hidden layers’ activations. Based on this observation, we note that the extra knowledge of uncertainty can come from the hidden layers of any white-box LLM that takes as input the  $(\mathbf{x}, \mathbf{y})$  pair, not necessarily from the LLM that generates  $(\mathbf{x}, \mathbf{y})$ . It is natural to start with the belief that the LLM which generates  $(\mathbf{x}, \mathbf{y})$  should have more information about the uncertainty of  $\mathbf{y}$ . However, any white-box LLM can output the hidden activations corresponding to  $(\mathbf{x}, \mathbf{y})$ .

Next, we formally present our supervised uncertainty calibration method for white-box, grey-box, and black-box LLMs.

**White-box supervised** uncertainty estimation (Wb-S): This Wb-S approach implements the method discussed in Section 3.1. It first constructs the features from both two sources and trains a supervised model to predict the uncertainty of the LLM’s responses.

**Grey-box supervised** uncertainty estimation (Gb-S): This Gb-S regime constructs the features only from the grey-box source, that is, those features relying on the probability and the entropy (such as those in Table 5 in Appendix C) but it ignores the hidden-layer activations.

Both the above two regimes consider one single LLM throughout the whole procedure. Specifically, the dataset  $\mathcal{D}_{\text{raw}}$  is generated based on the LLM  $p_\theta$ , and then features are extracted from  $\mathcal{D}_{\text{raw}}$  to construct  $\mathcal{D}_{\text{un}}$ . In particular, the feature extraction is based on the same LLM  $p_\theta$  as well and this assumes the full knowledge of  $p_\theta$  as the following diagram

$$\mathcal{D}_{\text{raw}} \xrightarrow{p_\theta} \mathcal{D}_{\text{un}}.$$

Then a supervised uncertainty estimation model is trained upon  $\mathcal{D}_{\text{un}}$ .

**Black-box supervised** uncertainty estimation (Bb-S): The Bb-S regime does not assume the knowledge of the parameters of  $p_\theta$  but still aims to estimate its uncertainty. To achieve this, it considers another open-source LLM denoted by  $q_\theta$ . The original data  $\mathcal{D}_{\text{raw}}$  is generated by  $p_\theta$  but then the uncertainty estimation data  $\mathcal{D}_{\text{un}}$  is constructed based on  $q_\theta$  from  $\mathcal{D}_{\text{raw}}$  as illustrated in the following diagram

$$\mathcal{D}_{\text{raw}} \xrightarrow{q_\theta} \mathcal{D}_{\text{un}}.$$

For example, for a prompt  $\mathbf{x}$ , a black-box LLM  $p_\theta$  generates the response  $\mathbf{y}$ . We utilize the open-source LLM  $q_\theta$  to treat  $(\mathbf{x}, \mathbf{y})$  jointly as a sequence of (prompt) tokens and extract the features of hidden activations and entropy as in Section 3.1. In this way, we use  $q_\theta$  together with the learned uncertainty model from  $\mathcal{D}_{\text{un}}$  to estimate the uncertainty of responses generated from  $p_\theta$  which we do not have any knowledge about.

---

**Algorithm 1** Supervised uncertainty estimation

---

**Input:** Target LLM  $p_\theta$  (the uncertainty of which is to be estimated), tool LLM  $q_\theta$  (used for uncertainty estimation), a labeled training dataset  $\mathcal{D}$ , a test sample with prompt  $\mathbf{x}$

1: %% Training phase:

2: Use  $p_\theta$  to generate responses for the samples in  $\mathcal{D}$  and construct the dataset  $\mathcal{D}_{\text{raw}}$

3: For each sample  $(\mathbf{x}_i, \mathbf{y}_i) \in \mathcal{D}_{\text{raw}}$ , extract features (hidden-layer activations, entropy- and probability-related features) using the LLM  $q_\theta$ , and then construct the dataset  $\mathcal{D}_{\text{un}}$

4: Train a supervised learning model  $\hat{g}$  that predicts  $z_i$  with  $\mathbf{v}_i$  based on the dataset  $\mathcal{D}_{\text{un}}$

5: %% Test phase:

6: Generate the response  $\mathbf{y}$  for the test prompt  $\mathbf{x}$

7: Extract features  $\mathbf{v}$  using  $q_\theta$

**Output:** Associate the response  $\mathbf{y}$  with the uncertainty score  $\hat{g}(\mathbf{v})$

---

Algorithm 1 summarizes our discussions so far on the supervised approach for uncertainty estimation. When the target LLM  $p_\theta = q_\theta$ , it corresponds to the first two regimes (white-box and grey-box). When the target LLM  $p_\theta \neq q_\theta$ , it corresponds to the third regime (black-box).

## 4 Numerical Experiments and Findings

In this section, we provide a systematic evaluation of the proposed supervised approach for estimating the uncertainty of the LLMs. All code used in our experiments is available at <https://github.com/LoveCatc/supervised-llm-uncertainty-estimation>.

### 4.1 LLMs, tasks, benchmarks, and performance metrics

Here we outline the general setup of the numerical experiments. Certain tasks may deviate from the general setup, and we will detail the specific adjustments as needed.

**LLMs.** For our numerical experiments, we mainly consider three open-source LLMs, LLaMA2-7B (Touvron et al., 2023), LLaMA3-8B (AI@Meta, 2024) and Gemma-7B (Gemma Team et al., 2024) as  $p_\theta$  defined in Section 2. For certain experiments, we also employ the models of LLaMA2-13B and Gemma-2B. We also use their respective tokenizers as provided by Hugging Face. We do not change the parameters/weights  $\theta$  of these LLMs.

**Tasks and Datasets.** We mainly consider three tasks for uncertainty estimation, question answering, multiple choice, and machine translation. All the labeled datasets for these tasks are in the form of  $\{(\mathbf{x}_i, \mathbf{y}_{i,\text{true}})\}_{i=1}^n$  where  $\mathbf{x}_i$  can be viewed as the prompt for the  $i$ -th sample and  $\mathbf{y}_{i,\text{true}}$  the true response. We adopt the few-shot prompting when generating the LLM’s response  $\mathbf{y}_i$ , and we use 5 examples in the prompt of the multiple-choice task and 3 examples for the remaining natural language generation tasks. This enables the LLM’s in-context learning ability (Radford et al., 2019; Zhang et al., 2023) and ensures the LLM’s responses are in a desirable format. We defer more details of the few-shot prompting to Appendix C.1. The three tasks are:

- Question answering. We follow Kuhn et al. (2023) and use the CoQA and TriviaQA (Joshi et al., 2017) datasets. The CoQA task requires the LLM to answer questions by understanding the provided text, and the TriviaQA requires the LLM to answer questions based on its pre-training knowledge. We adopt the scoring function  $s(\cdot, \cdot)$  as Rouge-1 (Lin and Och, 2004a) and label a response  $\mathbf{y}_i$  as correct if  $s(\mathbf{y}_i, \mathbf{y}_{i,\text{true}}) \geq 0.3$  and incorrect otherwise.
- Multiple choice. We consider the Massive Multitask Language Understanding (MMLU) dataset (Hendrycks et al., 2020), a collection of 15,858 questions covering 57 subjects across STEM. Due



to the special structure of the dataset, the generated output  $\mathbf{y}_i$  and the correct answer  $\mathbf{y}_{\text{true},i} \in \{A, B, C, D\}$ . Therefore, this task can also be regarded as a classification problem for the LLM by answering the question with one of the four candidate choices.

- **Machine translation.** We consider the WMT 2014 dataset (Bojar et al., 2014) for estimating LLM’s uncertainty on the machine translation task. The scoring function  $s(\cdot, \cdot)$  is chosen to be the BLEU score (Papineni et al., 2002; Lin and Och, 2004b) and the generated answer  $\mathbf{y}_i$  is labeled as correct if  $s(\mathbf{y}_i, \mathbf{y}_{i,\text{true}}) > 0.3$  and incorrect otherwise.

**Benchmarks.** We compare our approach with a number of the state-of-the-art benchmarks for the problem. Manakul et al. (2023) give a comprehensive survey of the existing methods and compare four distinct measures for predicting sentence generation uncertainty. The measures are based on either the maximum or average values of entropy or probability across the sentence, including Max Likelihood, Avg Likelihood, Max Ent, and Avg Ent defined in Table 5. We note that each of these measures can be applied as a single uncertainty estimator, and they are all applied in an unsupervised manner that does not require additional supervised training. In particular, in applying these measures for the MMLU dataset, since the answer only contains one token from  $\{A, B, C, D\}$ , we use the probabilities and the entropy (over these four tokens) as the benchmarks which represent the probability of the most likely choice and the entropy of all choices, respectively. Kuhn et al. (2023) generate multiple answers, compute their entropy in a semantic sense, and define the quantity as *semantic entropy*. This semantic-entropy uncertainty (SU) thus can be used as an uncertainty estimator for the LLM’s responses. Tian et al. (2023) propose the approach of asking the LLM for its confidence (denoted as A4U) which directly obtains the uncertainty score from the LLM itself.

**Our methods.** We follow the discussions in Section 3.4 and implement three versions of our proposed supervised approach: black-box supervised (Bb-S), grey-box supervised (Gb-S), and white-box supervised (Wb-S). These models have the same pipeline of training the uncertainty estimation model and the difference is only on the availability of the LLM. For the Bb-S method, we use the Gemma-7B as the model  $q_\theta$  to evaluate the uncertainty of LLaMA2-7B/LLaMA3-8B  $p_\theta$  (treated as a black-box), and reversely, use LLaMA2-7B to evaluate Gemma-7B. The supervised uncertainty model  $\hat{g}$  is trained based on the random forest model (Breiman, 2001). Details on the feature construction and the training of the random forest model are deferred to Appendix C.2.

**Performance metrics.** For the model evaluation, we follow Filos et al. (2019); Kuhn et al. (2023) and compare the performance of our methods against the benchmark using the generated uncertainty score to predict whether the answer is correct. The area under the receiver operator characteristic curve (AUROC) metric is employed to measure the performance of the uncertainty estimation. As discussed in Section 3.2, AUROC works as a good metric for the uncertainty estimation task whereas for the uncertainty calibration task, we follow the more standard calibration metrics and present the results in Section B.

## 4.2 Performance of uncertainty estimation

Now we present the performance on the uncertainty estimation task.

### 4.2.1 Question answering and machine translation

The question answering and machine translation tasks can all be viewed as natural language generation tasks so we present their results together. Table 1 summarizes the three versions of our proposed supervised method against the existing benchmarks in terms of AUROC.

Dataset	LLM	Benchmarks						Ours		
		MaxL	AvgL	MaxE	AvgE	SU	A4C	Bb-S	Gb-S	Wb-S
TriviaQA	G-7B	0.857	0.862	0.849	0.854	0.847	0.534	0.879	0.866	<b>0.882</b>
	L-7B	0.565	0.761	0.761	0.773	0.678	0.526	<b>0.925</b>	0.811	0.897
	L-8B	0.838	0.851	0.849	0.853	0.826	0.571	0.843	0.861	<b>0.874</b>
CoQA	G-7B	0.710	0.708	0.725	0.708	0.674	0.515	0.737	0.737	<b>0.762</b>
	L-7B	0.535	0.600	0.603	0.580	0.541	0.502	<b>0.848</b>	0.667	0.807
	L-8B	0.692	0.697	0.716	0.699	0.684	0.506	0.745	0.737	<b>0.769</b>
WMT-14	G-7B	0.668	0.589	0.637	0.811	0.572	0.596	<b>0.863</b>	0.829	0.855
	L-7B	0.606	0.712	0.583	0.711	0.513	0.506	<b>0.792</b>	0.724	0.779
	L-8B	0.554	0.685	0.616	0.729	0.510	0.502	0.700	0.724	<b>0.745</b>

Table 1: Out-of-sample AUROC performance for benchmarks and our methods on natural language generation tasks. G-7B, L-7B, and L-8B represent Gemma-7B, LLaMA2-7B, and LLaMA-8B, respectively. The columns MaxL, AvgL, MaxE, and AvgE all come from Manakul et al. (2023). The column SU implements the semantic uncertainty estimation by Kuhn et al. (2023), and the column A4C implements the ask-for-confidence method by Tian et al. (2023). The columns Bb-S, Gb-S, and Wb-S represent respectively the three regimes (black-box supervised, grey-box supervised, and white-box supervised) of our supervised method with details in Section 3.4.

We make several remarks on the numerical results. First, our methods generally have a better performance than the existing benchmarks. Note that the existing benchmarks are mainly unsupervised and based on one single score, and also that our method proceeds with the most standard pipeline for supervised training of an uncertainty estimation model. The advantage of our method should be attributed to the supervised nature and the labeled dataset. While these unsupervised benchmark methods can work in a larger scope than these NLP tasks (though they have not been extensively tested on open questions yet), our methods rely on the labeled dataset. But in addition to these better numbers, the experiment results show the potential of labeled datasets for understanding the uncertainty in LLM’s responses. In particular, our method Gb-S uses features including the benchmark methods, and it shows that some minor supervised training can improve a lot upon the ad-hoc uncertainty estimation based on one single score such as MaxL or MaxE.

Second, our method Wb-S has a clear advantage over our method Gb-S. Note that these two methods differ in that the Wb-S uses the hidden activations while the Gb-S only uses probability-related (and entropy-related) features. This implies that the hidden activations do contain uncertainty information which we will investigate more in Appendix A. Also, we note from the table that there is no single unsupervised grey-box method (under the Benchmarks columns) that consistently surpasses others across different datasets/NLP tasks. For example, among all these unsupervised benchmark methods for grey-box LLMs, AvgE emerges as a top-performing one for the Gemma-7B model when applied to the machine translation task, but it shows the poorest performance for the same Gemma-7B model when tested on the question-answering CoQA dataset. This inconsistency highlights some caveats when using the unsupervised approach for uncertainty estimation of LLMs.

Lastly, we note that the Bb-S method has a similar or even better performance as the Wb-S method. As discussed in Section 3.4, the performance of uncertainty estimation relies on the LLM that we use to evaluate the prompt-response pair. Therefore, it is not surprising to see that in the question-answering task, for answers generated by LLaMA2-7B, Bb-S features better uncertainty estimation than Wb-S, possibly because Gemma-7B, the LLM that is used as the “tool LLM” in Algorithm 1, encodes better knowledge about the uncertainty of the answers than LLaMA-7B. We also note that the performance of Bb-S is not always as good as Wb-S, and we hypothesize that it is because LLMs’ output distribution differs, which could result in evaluating the uncertainty of different answers. Despite these inconsistencies,

the performance of Bb-S is still strong, and these results point to a potential future avenue for estimating the uncertainty of closed-source LLMs.

#### 4.2.2 Multiple choice (MMLU)

Table 2 presents the performance of our methods against the benchmark methods on the MMLU dataset. For this multiple choice task, the output is from {A,B,C,D} which bears no semantic meaning, and therefore we do not include the Semantic Uncertainty (SU) as Table 1. The results show the advantage of our proposed supervised approach, consistent with the previous findings in Table 1.

Model	Benchmarks			Ours		
	Probability	Entropy	A4C	Bb-S	Gb-S	Wb-S
Gemma-7B	0.712	0.742	0.582	0.765	0.776	<b>0.833</b>
LLaMA2-7B	0.698	0.693	0.514	<b>0.732</b>	0.698	0.719
LLaMA3-8B	0.781	0.791	0.516	0.766	0.793	<b>0.830</b>

Table 2: Out-of-sample AUROC performance for benchmarks and our methods on the MMLU dataset. The columns Probability and Entropy come from Manakul et al. (2023), and the column A4C implements the ask-for-confidence method by Tian et al. (2023). The columns Bb-S, Gb-S, and Wb-S represent respectively the three regimes (black-box supervised, grey-box supervised, and white-box supervised) of our supervised method with details in Section 3.4.

We defer more numerical experiments and visualization to Appendices A and B where we investigate more on (i) the effect of the choice of layers; (ii) the scale of the LLMs used; (iii) the *uncertainty neurons* of the LLMs; and (iv) the calibration performance.

### 4.3 Transferability

In this subsection, we evaluate the robustness of our methods under the OOD setting.

**Setup for the OOD multiple-choice task.** We split the MMLU datasets into two groups based on the subjects: Group 1 contains questions from the first 40 subjects while Group 2 contains the remaining 17 subjects, such that the test dataset size of each group is similar (around 600 questions). Note that these 57 subjects span a diverse range of topics, and this means the training and test set can be very different. To test the OOD robustness, we train the proposed methods on one group and evaluate the performance on the other group.

**Setup for the OOD question-answering task.** For the QA task, since we have two datasets (CoQA and TriviaQA), we train the supervised model on either the TriviaQA or CoQA dataset and then evaluate its performance on the other dataset. While both datasets are for question-answering purposes, they diverge notably in two key aspects: (i) CoQA prioritizes assessing the LLM’s comprehension through the discernment of correct responses within extensive contextual passages, while TriviaQA focuses on evaluating the model’s recall of factual knowledge. (ii) TriviaQA typically contains answers comprising single words or short phrases, while CoQA includes responses of varying lengths, ranging from shorter to more extensive answers.

Table 3 summarizes the performance of these OOD experiments. As expected, for all the methods, there is a slight drop in terms of performance compared to the in-distribution setting (reported by the numbers in the parentheses in the table). We make the following observations based on the experiment results. First, based on the performance gap between in-distribution and OOD evaluation, it is evident that although incorporating white-box features such as hidden activations makes the model more susceptible to performance decreases on OOD tasks, these features also enhance the uncertainty estimation model’s overall capacity, and the benefits outweigh the drawbacks. It is also noteworthy that even

LLMs	Test data	Ours			Best of benchmarks	
		Bb-S	Gb-S	Wb-S	Best GB	Best BB
Transferability in MMLU						
G-7B	Group 1	0.756(0.768)	0.793(0.799)	0.846(0.854)	0.765	0.538
	Group 2	0.738(0.760)	0.755(0.754)	0.804(0.807)	0.721	0.616
L-7B	Group 1	0.733(0.749)	0.715(0.713)	0.726(0.751)	0.719	0.504
	Group 2	0.700(0.714)	0.676(0.677)	0.685(0.692)	0.679	0.529
L-8B	Group 1	0.763(0.773)	0.796(0.795)	0.836(0.839)	0.799	0.524
	Group 2	0.729(0.761)	0.786(0.785)	0.794(0.818)	0.782	0.507
Transferability in Question-Answering Datasets						
G-7B	TriviaQA	0.842(0.879)	0.861(0.866)	0.861(0.882)	0.862	0.847
	CoQA	0.702(0.737)	0.722(0.737)	0.730(0.762)	0.725	0.674
L-7B	TriviaQA	0.917(0.925)	0.801(0.811)	0.881(0.897)	0.773	0.678
	CoQA	0.825(0.848)	0.623(0.667)	0.764(0.807)	0.603	0.541
L-8B	TriviaQA	0.813(0.843)	0.859(0.861)	0.863(0.874)	0.853	0.826
	CoQA	0.710(0.745)	0.714(0.737)	0.725(0.769)	0.716	0.684

Table 3: Transferability of the trained uncertainty estimation model across different groups of subjects in MMLU and question-answering datasets. For our proposed Bb-S, Gb-S, and Wb-S methods, values within the parentheses ( $\cdot$ ) represent the AUROCs where the uncertainty estimation model is trained and tested on the same group of subjects or dataset, while values outside the parentheses represent models trained on another group of subjects or dataset. The Best GB and Best BB columns refer to the best AUROC achieved by the unsupervised grey-box baselines and black-box baselines (fully listed in Table 1 and Table 2), respectively.

in these scenarios of OOD, our Wb-S and Bb-S method almost consistently outperform corresponding baseline approaches. Overall, the robustness of our methods shows that the hidden layers’ activations within the LLM exhibit similar patterns in encoding uncertainty information to some extent. The performance drop (from in-distribution to OOD) observed in the MMLU dataset is notably less than that in the question-answering dataset, which may stem from the larger disparity between the CoQA and TriviaQA datasets compared to that between two distinct groups of subjects within the same MMLU dataset. This suggests that in cases of significant distributional shifts, re-training or re-calibrating the uncertainty estimation model using test data may be helpful.

## 5 Conclusions

In this paper, we study the problem of uncertainty estimation and calibration for LLMs. We follow a simple and standard supervised idea and use the labeled NLP datasets to train an uncertainty estimation model for LLMs. Our finding is that, first, the proposed supervised methods have better performances than the existing unsupervised methods. Second, the hidden activations of the LLMs contain uncertainty information about the LLMs’ responses. Third, the black-box regime of our approach (Bb-S) provides a new approach to estimating the uncertainty of closed-source LLMs. Lastly, we distinguish the task of uncertainty estimation from uncertainty calibration and show that a better uncertainty estimation model leads to better calibration performance. One limitation of our proposed supervised method is that it critically relies on the labeled data. For the scope of our paper, we restrict the discussion to the NLP tasks and datasets. One future direction is to utilize the human-annotated data for LLMs’ responses to train a supervised uncertainty estimation model for open-question prompts. We believe the findings that the supervised method gives a better performance and the hidden activations contain the uncertainty information will persist.

## References

- Abdar, Moloud, Farhad Pourpanah, Sadiq Hussain, Dana Rezazadegan, Li Liu, Mohammad Ghavamzadeh, Paul Fieguth, Xiaochun Cao, Abbas Khosravi, U Rajendra Acharya, et al. 2021. A review of uncertainty quantification in deep learning: Techniques, applications and challenges. *Information fusion* **76** 243–297.
- Ahdritz, Gustaf, Tian Qin, Nikhil Vyas, Boaz Barak, Benjamin L Edelman. 2024. Distinguishing the knowable from the unknowable with language models. *arXiv preprint arXiv:2402.03563* .
- AI@Meta. 2024. Llama 3 model card URL [https://github.com/meta-llama/llama3/blob/main/MODEL\\_CARD.md](https://github.com/meta-llama/llama3/blob/main/MODEL_CARD.md).
- Azaria, Amos, Tom Mitchell. 2023. The internal state of an llm knows when its lying. *arXiv preprint arXiv:2304.13734* .
- Bojar, Ondřej, Christian Buck, Christian Federmann, Barry Haddow, Philipp Koehn, Johannes Leveling, Christof Monz, Pavel Pecina, Matt Post, Herve Saint-Amand, et al. 2014. Findings of the 2014 workshop on statistical machine translation. *Proceedings of the ninth workshop on statistical machine translation*. 12–58.
- Breiman, Leo. 2001. Random forests. *Machine learning* **45** 5–32.
- Brown, Tom, Benjamin Mann, Nick Ryder, Melanie Subbiah, Jared D Kaplan, Prafulla Dhariwal, Arvind Neelakantan, Pranav Shyam, Girish Sastry, Amanda Askell, et al. 2020. Language models are few-shot learners. *Advances in neural information processing systems* **33** 1877–1901.
- Bubeck, Sébastien, Varun Chandrasekaran, Ronen Eldan, Johannes Gehrke, Eric Horvitz, Ece Kamar, Peter Lee, Yin Tat Lee, Yuanzhi Li, Scott Lundberg, et al. 2023. Sparks of artificial general intelligence: Early experiments with gpt-4. *arXiv preprint arXiv:2303.12712* .
- Burns, Collin, Haotian Ye, Dan Klein, Jacob Steinhardt. 2022. Discovering latent knowledge in language models without supervision. *arXiv preprint arXiv:2212.03827* .
- CH-Wang, Sky, Benjamin Van Durme, Jason Eisner, Chris Kedzie. 2023. Do androids know they’re only dreaming of electric sheep? *arXiv preprint arXiv:2312.17249* .
- Chen, Chao, Kai Liu, Ze Chen, Yi Gu, Yue Wu, Mingyuan Tao, Zhihang Fu, Jieping Ye. 2024. Inside: Llms’ internal states retain the power of hallucination detection. *arXiv preprint arXiv:2402.03744* .
- Desai, Shrey, Greg Durrett. 2020. Calibration of pre-trained transformers. *arXiv preprint arXiv:2003.07892* .
- Duan, Hanyu, Yi Yang, Kar Yan Tam. 2024. Do llms know about hallucination? an empirical investigation of llm’s hidden states. *arXiv preprint arXiv:2402.09733* .
- Duan, Jinhao, Hao Cheng, Shiqi Wang, Chenan Wang, Alex Zavalny, Renjing Xu, Bhavya Kailkhura, Kaidi Xu. 2023. Shifting attention to relevance: Towards the uncertainty estimation of large language models. *arXiv preprint arXiv:2307.01379* .
- Farquhar, Sebastian, Jannik Kossen, Lorenz Kuhn, Yarin Gal. 2024. Detecting hallucinations in large language models using semantic entropy. *Nature* **630**(8017) 625–630.

- Filos, Angelos, Sebastian Farquhar, Aidan N Gomez, Tim GJ Rudner, Zachary Kenton, Lewis Smith, Milad Alizadeh, Arnoud de Kroon, Yarin Gal. 2019. Benchmarking bayesian deep learning with diabetic retinopathy diagnosis. *Preprint at <https://arxiv.org/abs/1912.10481>* .
- Fomicheva, Marina, Shuo Sun, Lisa Yankovskaya, Frédéric Blain, Francisco Guzmán, Mark Fishel, Nikolaos Aletras, Vishrav Chaudhary, Lucia Specia. 2020. Unsupervised quality estimation for neural machine translation. *Transactions of the Association for Computational Linguistics* **8** 539–555.
- Gawlikowski, Jakob, Cedric Rovee Njietcheu Tassi, Mohsin Ali, Jongseok Lee, Matthias Humt, Jianxiang Feng, Anna Kruspe, Rudolph Triebel, Peter Jung, Ribana Roscher, et al. 2023. A survey of uncertainty in deep neural networks. *Artificial Intelligence Review* **56**(Suppl 1) 1513–1589.
- Gemma Team, Thomas Mesnard, Cassidy Hardin, Robert Dadashi, Surya Bhupatiraju, Laurent Sifre, Morgane Rivière, Mihir Sanjay Kale, Juliette Love, Pouya Tafti, Léonard Hussenot, et al. 2024. Gemma doi:10.34740/KAGGLE/M/3301. URL <https://www.kaggle.com/m/3301>.
- Guo, Chuan, Geoff Pleiss, Yu Sun, Kilian Q Weinberger. 2017. On calibration of modern neural networks. *International conference on machine learning*. PMLR, 1321–1330.
- Hendrycks, Dan, Collin Burns, Steven Basart, Andy Zou, Mantas Mazeika, Dawn Song, Jacob Steinhardt. 2020. Measuring massive multitask language understanding. *arXiv preprint arXiv:2009.03300* .
- Hou, Bairu, Yujian Liu, Kaizhi Qian, Jacob Andreas, Shiyu Chang, Yang Zhang. 2023. Decomposing uncertainty for large language models through input clarification ensembling. *arXiv preprint arXiv:2311.08718* .
- Joshi, Mandar, Eunsol Choi, Daniel S Weld, Luke Zettlemoyer. 2017. Triviaqa: A large scale distantly supervised challenge dataset for reading comprehension. *arXiv preprint arXiv:1705.03551* .
- Kadavath, Saurav, Tom Conerly, Amanda Askell, Tom Henighan, Dawn Drain, Ethan Perez, Nicholas Schiefer, Zac Hatfield-Dodds, Nova DasSarma, Eli Tran-Johnson, et al. 2022. Language models (mostly) know what they know. *arXiv preprint arXiv:2207.05221* .
- Kuhn, Lorenz, Yarin Gal, Sebastian Farquhar. 2023. Semantic uncertainty: Linguistic invariances for uncertainty estimation in natural language generation. *arXiv preprint arXiv:2302.09664* .
- Kumar, Bhawesh, Charlie Lu, Gauri Gupta, Anil Palepu, David Bellamy, Ramesh Raskar, Andrew Beam. 2023. Conformal prediction with large language models for multi-choice question answering. *arXiv preprint arXiv:2305.18404* .
- Li, Kenneth, Oam Patel, Fernanda Viégas, Hanspeter Pfister, Martin Wattenberg. 2024. Inference-time intervention: Eliciting truthful answers from a language model. *Advances in Neural Information Processing Systems* **36**.
- Lin, Chin-Yew, Franz Josef Och. 2004a. Automatic evaluation of machine translation quality using longest common subsequence and skip-bigram statistics. *Proceedings of the 42nd annual meeting of the association for computational linguistics (ACL-04)*. 605–612.
- Lin, Chin-Yew, Franz Josef Och. 2004b. ORANGE: a method for evaluating automatic evaluation metrics for machine translation. *COLING 2004: Proceedings of the 20th International Conference on Computational Linguistics*. COLING, Geneva, Switzerland, 501–507. URL <https://www.aclweb.org/anthology/C04-1072>.

- Lin, Zhen, Shubhendu Trivedi, Jimeng Sun. 2023. Generating with confidence: Uncertainty quantification for black-box large language models. *arXiv preprint arXiv:2305.19187* .
- Lin, Zi, Jeremiah Zhe Liu, Jingbo Shang. 2022. Towards collaborative neural-symbolic graph semantic parsing via uncertainty. *Findings of the Association for Computational Linguistics: ACL 2022* .
- Liu, Kevin, Stephen Casper, Dylan Hadfield-Menell, Jacob Andreas. 2023. Cognitive dissonance: Why do language model outputs disagree with internal representations of truthfulness? *arXiv preprint arXiv:2312.03729* .
- Malinin, Andrey, Mark Gales. 2021. Uncertainty estimation in autoregressive structured prediction. *International Conference on Learning Representations*. URL <https://openreview.net/forum?id=jN5y-zb5Q7m>.
- Manakul, Potsawee, Adian Liusie, Mark JF Gales. 2023. Selfcheckgpt: Zero-resource black-box hallucination detection for generative large language models. *arXiv preprint arXiv:2303.08896* .
- Mielke, Sabrina J, Arthur Szlam, Emily Dinan, Y-Lan Boureau. 2022. Reducing conversational agents’ overconfidence through linguistic calibration. *Transactions of the Association for Computational Linguistics* **10** 857–872.
- Mohri, Christopher, Tatsunori Hashimoto. 2024. Language models with conformal factuality guarantees. *arXiv preprint arXiv:2402.10978* .
- Ouyang, Long, Jeffrey Wu, Xu Jiang, Diogo Almeida, Carroll Wainwright, Pamela Mishkin, Chong Zhang, Sandhini Agarwal, Katarina Slama, Alex Ray, et al. 2022. Training language models to follow instructions with human feedback. *Advances in neural information processing systems* **35** 27730–27744.
- Papineni, Kishore, Salim Roukos, Todd Ward, Wei jing Zhu. 2002. Bleu: a method for automatic evaluation of machine translation. 311–318.
- Pedregosa, Fabian, Gaël Varoquaux, Alexandre Gramfort, Vincent Michel, Bertrand Thirion, Olivier Grisel, Mathieu Blondel, Peter Prettenhofer, Ron Weiss, Vincent Dubourg, et al. 2011. Scikit-learn: Machine learning in python. *the Journal of machine Learning research* **12** 2825–2830.
- Platt, John, et al. 1999. Probabilistic outputs for support vector machines and comparisons to regularized likelihood methods. *Advances in large margin classifiers* **10**(3) 61–74.
- Plaut, Benjamin, Khanh Nguyen, Tu Trinh. 2024. Softmax probabilities (mostly) predict large language model correctness on multiple-choice q&a. *arXiv preprint arXiv:2402.13213* .
- Quach, Victor, Adam Fisch, Tal Schuster, Adam Yala, Jae Ho Sohn, Tommi S Jaakkola, Regina Barzilay. 2023. Conformal language modeling. *arXiv preprint arXiv:2306.10193* .
- Radford, Alec, Jeffrey Wu, Rewon Child, David Luan, Dario Amodei, Ilya Sutskever, et al. 2019. Language models are unsupervised multitask learners. *OpenAI blog* **1**(8) 9.
- Rawte, Vipula, Amit Sheth, Amitava Das. 2023. A survey of hallucination in large foundation models. *arXiv preprint arXiv:2309.05922* .
- Si, Chenglei, Chen Zhao, Sewon Min, Jordan Boyd-Graber. 2022. Re-examining calibration: The case of question answering. *arXiv preprint arXiv:2205.12507* .

- Slobodkin, Aviv, Omer Goldman, Avi Caciularu, Ido Dagan, Shauli Ravfogel. 2023. The curious case of hallucinatory (un) answerability: Finding truths in the hidden states of over-confident large language models. *Proceedings of the 2023 Conference on Empirical Methods in Natural Language Processing*. 3607–3625.
- Su, Weihang, Changyue Wang, Qingyao Ai, Yiran Hu, Zhijing Wu, Yujia Zhou, Yiqun Liu. 2024. Unsupervised real-time hallucination detection based on the internal states of large language models. *arXiv preprint arXiv:2403.06448* .
- Tian, Katherine, Eric Mitchell, Allan Zhou, Archit Sharma, Rafael Rafailov, Huaxiu Yao, Chelsea Finn, Christopher D Manning. 2023. Just ask for calibration: Strategies for eliciting calibrated confidence scores from language models fine-tuned with human feedback. *arXiv preprint arXiv:2305.14975* .
- Touvron, Hugo, Louis Martin, Kevin Stone, Peter Albert, Amjad Almahairi, Yasmine Babaei, Nikolay Bashlykov, Soumya Batra, Prajjwal Bhargava, Shruiti Bhosale, et al. 2023. Llama 2: Open foundation and fine-tuned chat models. *arXiv preprint arXiv:2307.09288* .
- Verma, Shreyas, Kien Tran, Yusuf Ali, Guangyu Min. 2023. Reducing llm hallucinations using epistemic neural networks. *arXiv preprint arXiv:2312.15576* .
- Xu, Ziwei, Sanjay Jain, Mohan Kankanhalli. 2024. Hallucination is inevitable: An innate limitation of large language models. *arXiv preprint arXiv:2401.11817* .
- Ye, Xi, Greg Durrett. 2021. Can explanations be useful for calibrating black box models? *arXiv preprint arXiv:2110.07586* .
- Zadrozny, Bianca, Charles Elkan. 2002. Transforming classifier scores into accurate multiclass probability estimates. *Proceedings of the eighth ACM SIGKDD international conference on Knowledge discovery and data mining*. 694–699.
- Zhang, Hanlin, Yi-Fan Zhang, Yaodong Yu, Dhruv Madeka, Dean Foster, Eric Xing, Hima Lakkaraju, Sham Kakade. 2023. A study on the calibration of in-context learning. *arXiv preprint arXiv:2312.04021* .
- Zhang, Shujian, Chengyue Gong, Eunsol Choi. 2021. Knowing more about questions can help: Improving calibration in question answering. *arXiv preprint arXiv:2106.01494* .

## A Interpreting the Uncertainty Estimation

Now we use some visualizations to provide insights into the working mechanism of the uncertainty estimation procedure for LLMs and to better understand the experiment results in the previous subsection.

### A.1 Layer comparison

For general LLMs, each token is associated with a relatively large number of hidden layers (32 layers for LLaMA2-7B for example), each of which is represented by high-dimensional vectors (4096 for LLaMA2-7B). Thus it is generally not a good practice to incorporate all hidden layers as features for the uncertainty estimation due to this dimensionality. Previous works find that the middle layer and the last layer activations of the LLM’s last token contain the most useful features for supervised learning (Burns et al., 2022; Chen et al., 2024; Ahdritz et al., 2024; Azaria and Mitchell, 2023). To investigate the layer-wise effect for uncertainty estimation, we implement our Wb-S method with features different in two



aspects: (i) different layers within the LLM architecture, specifically focusing on the middle and last layers (e.g., LLaMA2-7B and LLaMA3-8B: 16th and 32nd layers out of 32 layers with 4096 dimensions; Gemma-7B: 14th and 28th layers out of 28 layers with 3072 dimensions); and (ii) position of token activations, including averaging hidden activations over all the prompt/answer tokens or utilizing the hidden activation of the last token. The second aspect makes sense when the output contains more than one token, so we conduct this experiment on the natural language generation tasks only. Figure 1 gives a visualization of the comparison result. While the performances of these different feature extraction ways are quite similar in terms of performance across different tasks and LLMs, activation features from the middle layer generally perform better than the last layer. This may come from the fact that the last layer focuses more on the generation of the next token instead of summarizing information of the whole sentence, as has been discussed by [Azaria and Mitchell \(2023\)](#).

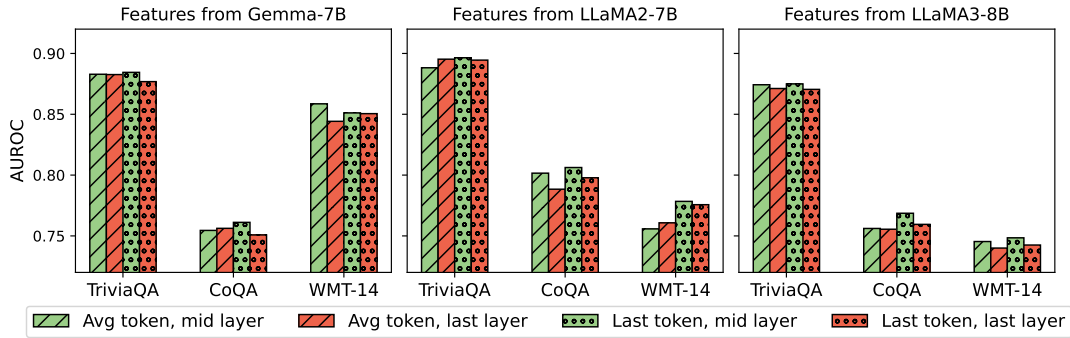


Figure 1: Performance comparison of using hidden activations from different tokens and layers as features in the Wb-S method. The bars filled with ‘/’ and ‘.’ represent the activations averaged over the answer tokens and the hidden activation of the last token, respectively. And the green and orange bars denote the activations from the middle and the last layer, respectively.

## A.2 Scaling effect

In Figure 2, we investigate whether larger LLMs’ hidden activations enhance our uncertainty estimation method. For a fair comparison, we fix the target LLM that generates the output in Algorithm 1 and vary the tool LLM used for analysis. For example, in the left plot of Figure 2, we use Gemma-7B to generate the outputs, and LLaMA2-7B, LLaMA2-13B, and Gemma-7B to perform uncertainty estimation.

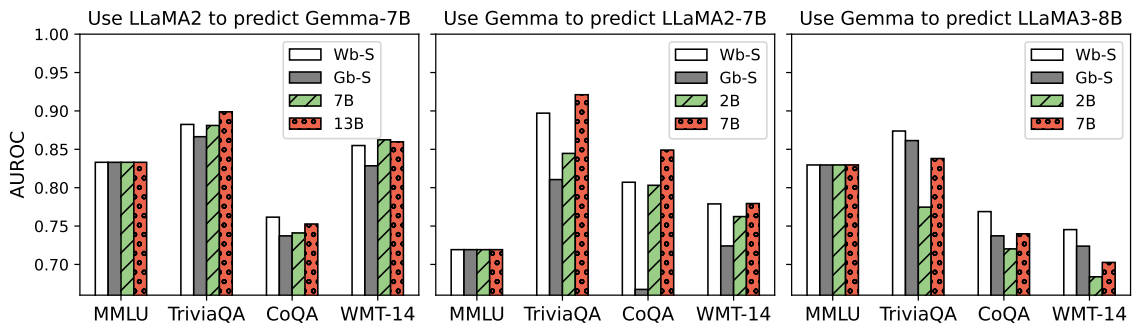


Figure 2: (Left) Using the hidden activations of LLaMA2-7B and LLaMA2-13B to estimate the uncertainty of the answer provided by Gemma-7B. (Middle) Using the hidden activations of Gemma-2B and Gemma-7B to estimate the uncertainty of the answer provided by LLaMA2-7B. (Right) Using the hidden activations of Gemma-2B and Gemma-7B to estimate the uncertainty of the answer provided by LLaMA3-8B

We find that larger LLM does encode better knowledge about the uncertainty, which is attributed

to their improved knowledge in answering the questions. We also note that in the case of using Gemma to predict LLaMA2-7B, even a small tool LLM (Gemma-2B) is capable of achieving better performance than the Gb-S that only uses the entropy- and probability-related features from the target LLM. This result also underscores the benefits of adopting the internal state in estimating the uncertainty, even from an LLM different from the one generating the answers.

### A.3 Histogram of correlations

Figure 3 plots the histograms of the pairwise correlations between the neuron activations and the labels (whether the LLM’s response is correct). We make two observations here: First, for both LLMs, some neurons have a significantly positive (or negative) correlation with the label. We can interpret these neurons as the *uncertainty neuron* for the corresponding task. When these neurons are activated, the LLMs are uncertain about their responses. Second, Gemma-7B and LLaMA3-8B have more significant neurons than LLaMA2-7B, and this is consistent with the better performance of Gemma-7B and LLaMA3-8B in Table 1 and Table 2. Also, this reinforces that the hidden activations of the LLMs contain uncertainty information about the LLM’s output.

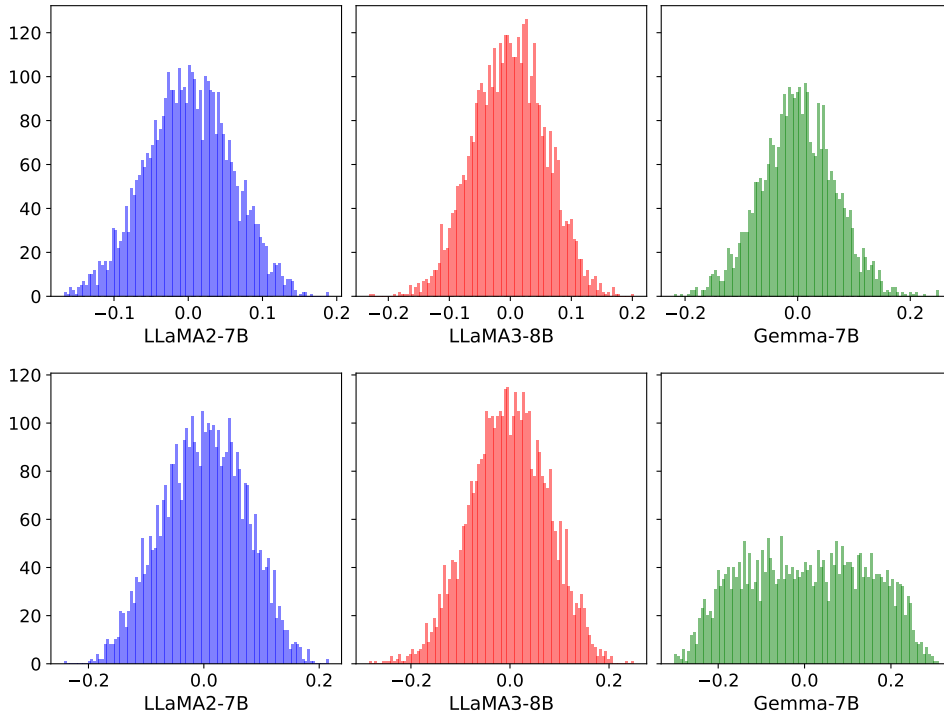


Figure 3: The histograms of the pairwise correlations on the TriviaQA task between the neuron activations and the labels (whether the LLM’s response is correct), where the neural values are the last-token hidden activations of answers from the middle layer (upper) and the last layer (lower) of two models respectively.

Figure 4 plots some example neurons’ activation by selecting the neurons with the largest absolute correlations in Figure 3. More neurons from the last layer can be found in Figure 5. These neurons as an individual indicator exhibit different distributional patterns when the response is correct compared to when the response is incorrect, and thus reflect the uncertainty of the LLM’s responses.

### A.4 Proof of Proposition 3.1

The proof of Proposition 3.1 follows from the definition of  $f^*$ .

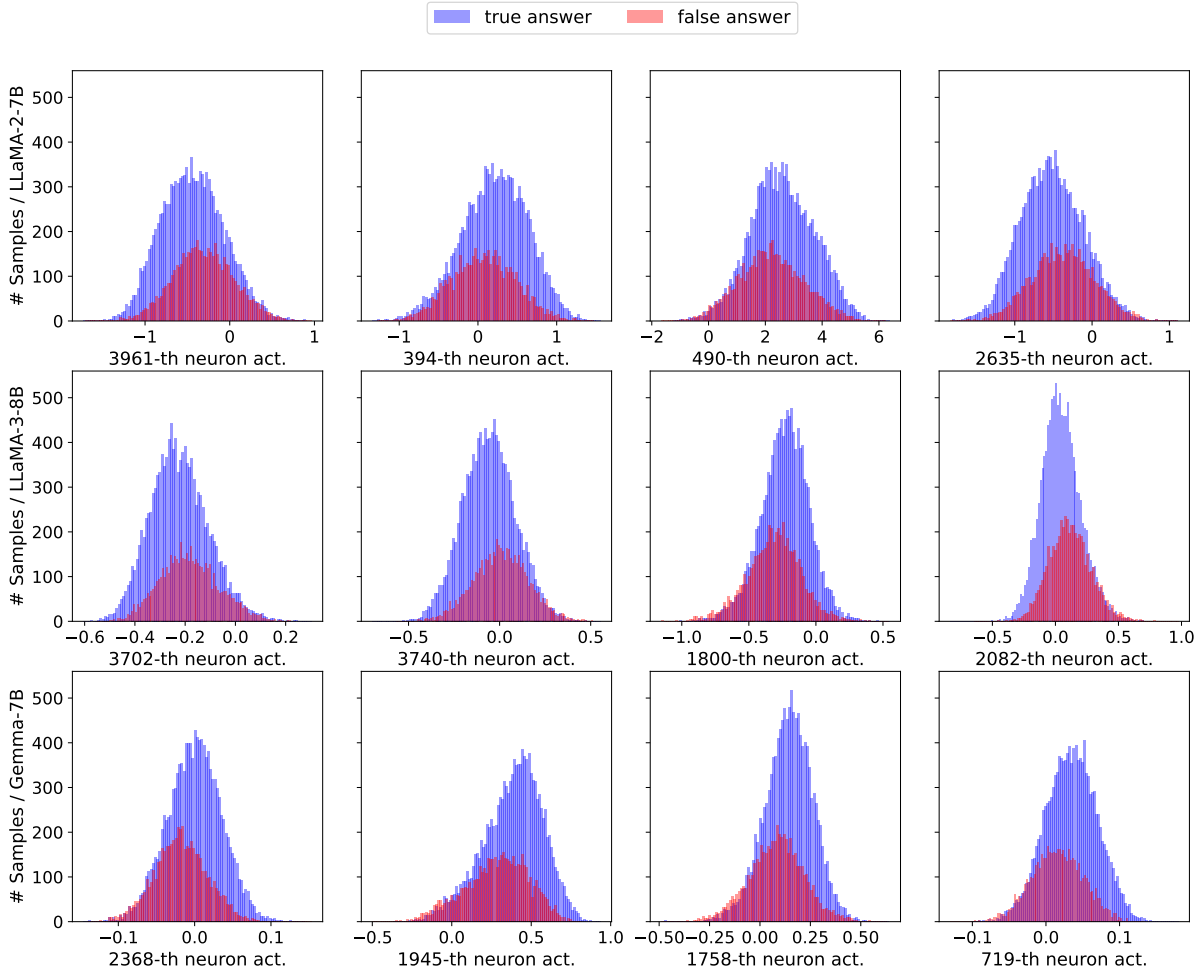


Figure 4: Distribution of values from particular neurons of mid-layers on TriviaQA dataset.

## B Calibration performance

In Section 3.2, we distinguish the two tasks of uncertainty estimation and uncertainty calibration. Throughout the paper, we have been focused on improving the performance on the task of uncertainty estimation – to predict when the LLM is uncertain about its response. Generally, a better uncertainty estimation model leads to one with better calibration performance. The calibration (or recalibration) of the uncertainty estimation model can be indeed reduced to the classic ML setting which does not involve the LLM. Table 4 gives the calibration performance and we see an advantage of our supervised methods over benchmark methods consistent with the AUROC performance in Table 1. We adopt the histogram binning method here because we find that the temperature scaling method and the Platt scaling method will give all predicted scores concentrated within a small range such as  $[0.2, 0.6]$ . We also do not exclude the possibility that the other calibration methods can give even better performance. The point to make here is that uncertainty estimation and uncertainty calibration are two closely related tasks. Note that (i) a better uncertainty estimation model leads to a better calibration performance and (ii) the LLMs are pretrained and not designed for these NLP tasks in the first place (see Section 3.3) so that there is no uncertainty score readily available (as the predicted probabilities for the image classifiers); we emphasize the importance of an extra uncertainty estimation procedure as our supervised one so to extract the uncertainty information from the inside of the LLMs.

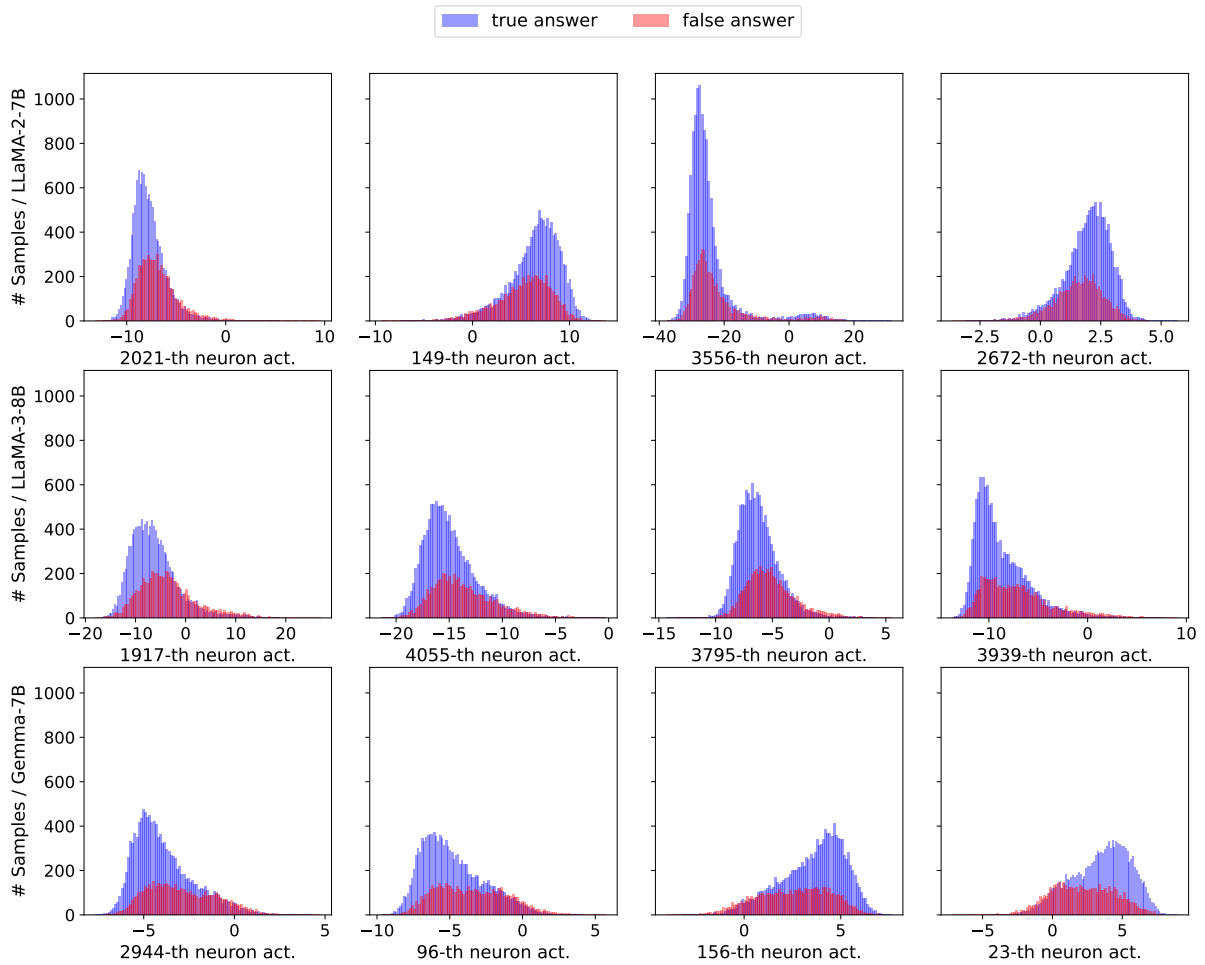


Figure 5: More distribution of values from specific neurons of last layers on the TriviaQA dataset. The plots are obtained in the same way as Figure 4.

Metric	Dataset	Model	Benchmarks						Ours		
			MaxL	AvgL	MaxE	AvgE	SU	A4C	Bb-S	Gb-S	Wb-S
NLL	TriviaQA	G-7B	0.478	0.500	0.428	0.472	0.739	8.710	0.414	0.467	0.392
		L-7B	1.155	0.551	0.575	0.600	1.481	21.119	0.338	0.580	0.388
		L-8B	0.483	0.407	0.383	0.401	0.719	8.515	0.423	0.467	0.365
	CoQA	G-7B	0.778	0.474	0.469	0.476	0.632	8.106	0.474	0.497	0.457
		L-7B	1.047	0.620	0.637	0.649	1.358	11.708	0.417	0.607	0.457
		L-8B	0.823	0.502	0.508	0.499	0.762	8.007	0.551	0.535	0.507
	WMT-14	G-7B	9.674	1.266	0.809	0.618	0.701	17.933	0.454	0.463	0.449
		L-7B	1.204	1.150	0.718	0.809	0.796	16.913	0.553	0.622	0.583
		L-8B	1.490	0.752	0.652	0.676	0.722	21.340	0.649	0.673	0.612
ECE	TriviaQA	G-7B	0.152	0.138	0.066	0.115	0.275	0.253	0.056	0.075	0.067
		L-7B	0.437	0.068	0.048	0.146	0.188	0.616	0.043	0.087	0.049
		L-8B	0.171	0.082	0.046	0.081	0.196	0.283	0.107	0.087	0.075
	CoQA	G-7B	0.356	0.054	0.112	0.064	0.221	0.237	0.121	0.129	0.113
		L-7B	0.397	0.065	0.105	0.073	0.174	0.494	0.052	0.071	0.038
		L-8B	0.339	0.031	0.071	0.033	0.196	0.312	0.156	0.110	0.122
	WMT-14	G-7B	0.499	0.464	0.234	0.197	0.072	0.521	0.097	0.063	0.073
		L-7B	0.164	0.389	0.065	0.269	0.127	0.491	0.045	0.090	0.101
		L-8B	0.318	0.192	0.051	0.142	0.029	0.618	0.145	0.201	0.137
Brier	TriviaQA	G-7B	0.282	0.221	0.224	0.215	0.344	0.279	0.266	0.288	0.282
		L-7B	0.431	0.241	0.271	0.259	0.322	0.645	0.334	0.322	0.315
		L-8B	0.262	0.192	0.204	0.188	0.291	0.373	0.258	0.265	0.255
	CoQA	G-7B	0.318	0.174	0.188	0.171	0.232	0.241	0.207	0.218	0.212
		L-7B	0.395	0.233	0.242	0.230	0.265	0.464	0.296	0.256	0.276
		L-8B	0.338	0.197	0.201	0.191	0.255	0.359	0.258	0.242	0.248
	WMT-14	G-7B	0.505	0.454	0.330	0.319	0.247	0.606	0.327	0.287	0.309
		L-7B	0.313	0.413	0.271	0.334	0.275	0.502	0.296	0.277	0.288
		L-8B	0.343	0.279	0.250	0.263	0.246	0.620	0.282	0.300	0.284

Table 4: Calibration performance on natural language generation tasks after histogram binning. The base models are from Table 1. The original uncertainty scores from the base models are first scaled into  $[0, 1]$  and then a histogram binning is performed with 20 bins of equal length.

## C Details for the Numerical Experiments

We ran all of our experiments on an AMD EPYC 7452 128-core processor with 4×48G NVIDIA A6000 GPUs.

### C.1 Dataset preparation

In the following we provide more information for the three tasks considered in our numerical experiments.

- Question answering. We follow [Kuhn et al. \(2023\)](#) and use the CoQA and TriviaQA ([Joshi et al., 2017](#)) datasets. The CoQA task requires the LLM to answer questions by understanding the provided text, and the TriviaQA requires the LLM to answer questions based on its pre-training knowledge. We adopt the scoring function  $s(\cdot, \cdot)$  as Rouge-1 ([Lin and Och, 2004a](#)) and label a response  $\mathbf{y}_i$  as correct if  $s(\mathbf{y}_i, \mathbf{y}_{i,\text{true}}) \geq 0.3$  and incorrect otherwise.
- Multiple choice. We consider the Massive Multitask Language Understanding (MMLU) dataset ([Hendrycks et al., 2020](#)), a collection of 15,858 questions covering 57 subjects across STEM. Due to the special structure of the dataset, the generated output  $\mathbf{y}_i$  and the correct answer  $\mathbf{y}_{\text{true},i} \in \{A, B, C, D\}$ . Therefore, this task can also be regarded as a classification problem for the LLM by answering the question with one of the four candidate choices.
- Machine translation. We consider the WMT 2014 dataset ([Bojar et al., 2014](#)) for estimating LLM’s uncertainty on the machine translation task. The scoring function  $s(\cdot, \cdot)$  is chosen to be the BLEU

score (Papineni et al., 2002; Lin and Och, 2004b) and the generated answer  $\mathbf{y}_i$  is labeled as correct if  $s(\mathbf{y}_i, \mathbf{y}_{i,\text{true}}) > 0.3$  and incorrect otherwise.

**Prompt dataset generation.** For all the tasks studied in this paper, we adopt the few-shot prompting for the LLM. Specifically, in the prompt, we provide  $r$  examples to make the LLM learn the format of the response, as illustrated in the following. For the question-answering task, we construct the prompt without using any question-answering sample repeatedly in the original dataset. For example, Prompt 1 includes the 1st to  $r$ -th question-answering samples in the original dataset as the examples and the  $(r + 1)$ -th sample as the target question-answering pair for the LLM; next, Prompt 2 uses the  $(r + 2)$ -th to  $(2r + 1)$ -th samples as the examples and the  $(2r + 2)$ -th sample as the target question-answering pair. However, as the test datasets of MMLU and WMT used for evaluation are not sufficiently large, we generate the prompt in a convolution-like manner: Prompt 2 includes the 2nd to  $(r + 1)$ -th question-answering samples as the examples and the  $(r + 2)$ -th sample as the target question-answering pair.

**Dataset split.** After generating the prompt-answering dataset, we split this dataset into two parts for training the calibration model and evaluation/test. For the MMLU and WMT datasets, we take the dataset generated from the original validation/test dataset. For the question-answering task, as the answer of TriviaQA in the original test dataset is vacant, we take the first 2000 generated prompt-answering pairs from the training dataset as the test dataset, and the remaining for training.

**Prompting format.** Here we give the different prompting templates used for different tasks. We use few-shot prompting and the templates can always be roughly divided into four parts: introduction (empty only for WMT), examples, question, and answer, where examples are just  $r$  distinct question-answer pairs in the same form as the question and answer parts. We feed the model with the template string except for the reference answer as inputs.

#### COQA

Reading the passage and answer given questions accordingly.

Passage:  $\{a\ \text{passage in COQA}\}$

Examples:

$\{r\ \text{distinct QA pairs related to the given passage}\}$

Q:  $\{a\ \text{new question related to the given passage}\}$

A:  $\{reference\ \text{answer}\}$

#### TriviaQA

Answer the question as following examples.

Examples:

$\{r\ \text{distinct QA pairs}\}$

Q:  $\{a\ \text{new question}\}$

A:  $\{reference\ \text{answer}\}$

### MMLU

You would be given a multiple-choice question paired with 4 choices (A-D). Choose one of them using letter A, B, C, or D as the correct answer to the question. Here are some examples:

{*r distinct QA pairs*}

Now answer the question:

{*a new question*}

A: {*answer sentence A*}

B: {*answer sentence B*}

C: {*answer sentence C*}

D: {*answer sentence D*}

Answer: {*reference answer (a letter)*}

### WMT

{*r distinct QA pairs*}

Q: What is the English translation of the following sentence? {*a French sentence*}

A: {*reference answer (an English sentence)*}

## C.2 Details of the training procedure

For the three regimes of our supervised approach presented in Section 3.4, the details of the supervised training procedure are as below:

**Gb-S.** For the natural language generation tasks (question-answering and machine-translation), we train a random forest model with the input features listed in Table 5 (20 features in total). For the multiple-choice task, as the answer has only one token from {A, B, C, D}, we take the output logits of these 4 tokens (denoted as  $\alpha_A$ ,  $\alpha_B$ ,  $\alpha_C$ , and  $\alpha_D$ ) after inputting the question prompt  $\mathbf{x}$  to the LLM. Then, we get the probability of each choice as follows:

$$p_\theta(y|\mathbf{x}) = \frac{\exp(\alpha_y)}{\sum_{y' \in \{A, B, C, D\}} \exp(\alpha_{y'})}, \forall y \in \{A, B, C, D\}.$$

Then we use 5 features as the input to Gb-S: the entropy of this distribution, and the sorted probability values in descending order.

Name	Features from the response/answer	Features from the prompt/question
Max Ent	$\max_{j \in \{1, \dots, m\}} H(p_\theta(\cdot   \mathbf{x}, \mathbf{y}_{1:j-1}))$	$\max_{j \in \{1, \dots, n\}} H(p_\theta(\cdot   \mathbf{x}_{1:j-1}))$
Min Ent	$\min_{j \in \{1, \dots, m\}} H(p_\theta(\cdot   \mathbf{x}, \mathbf{y}_{1:j-1}))$	$\min_{j \in \{1, \dots, n\}} H(p_\theta(\cdot   \mathbf{x}_{1:j-1}))$
Avg Ent	$\frac{1}{m} \sum_{j=1}^m H(p_\theta(\cdot   \mathbf{x}, \mathbf{y}_{1:j-1}))$	$\frac{1}{n} \sum_{j=1}^n H(p_\theta(\cdot   \mathbf{x}_{1:j-1}))$
Std Ent	$\sqrt{\frac{\sum_{j=1}^m (H(p_\theta(\cdot   \mathbf{x}, \mathbf{y}_{1:j-1})) - \text{Avg Ent})^2}{m-1}}$	$\sqrt{\frac{\sum_{j=1}^n (H(p_\theta(\cdot   \mathbf{x}_{1:j-1})) - \text{Avg Ent})^2}{n-1}}$
Max Likelihood	$\max_{j \in \{1, \dots, m\}} -\log p_\theta(y_j   \mathbf{x}, \mathbf{y}_{1:j-1})$	$\max_{j \in \{1, \dots, n\}} -\log p_\theta(x_j   \mathbf{x}_{1:j-1})$
Min Likelihood	$\min_{j \in \{1, \dots, m\}} -\log p_\theta(y_j   \mathbf{x}, \mathbf{y}_{1:j-1})$	$\min_{j \in \{1, \dots, n\}} -\log p_\theta(x_j   \mathbf{x}_{1:j-1})$
Avg Likelihood	$\frac{1}{m} \sum_{j=1}^m -\log p_\theta(y_j   \mathbf{x}, \mathbf{y}_{1:j-1})$	$\frac{1}{n} \sum_{j=1}^n -\log p_\theta(x_j   \mathbf{x}_{1:j-1})$
Std Likelihood	$\sqrt{\frac{\sum_{j=1}^m (-\log p_\theta(y_j   \mathbf{x}, \mathbf{y}_{1:j-1}) - \text{Avg Likelihood})^2}{m-1}}$	$\sqrt{\frac{\sum_{j=1}^n (-\log p_\theta(x_j   \mathbf{x}_{1:j-1}) - \text{Avg Likelihood})^2}{n-1}}$
Avg Prob	$\frac{1}{m} \sum_{j=1}^m p_\theta(y_j   \mathbf{x}, \mathbf{y}_{1:j-1})$	$\frac{1}{n} \sum_{j=1}^n p_\theta(x_j   \mathbf{x}_{1:j-1})$
Std Prob	$\sqrt{\frac{\sum_{j=1}^m (p_\theta(y_j   \mathbf{x}, \mathbf{y}_{1:j-1}) - \text{Avg Prob})^2}{m-1}}$	$\sqrt{\frac{\sum_{j=1}^n (p_\theta(x_j   \mathbf{x}_{1:j-1}) - \text{Avg Prob})^2}{n-1}}$

Table 5: Grey-box features used for the supervised task of uncertainty estimation for LLMs.

**Wb-S.** The dimension of a hidden layer from LM is typically high (e.g., 4096 for LLaMA2-7B), which

may prevent the calibration model from capturing the effective uncertainty information revealed from the activations, especially with limited training samples. Thus, before training a model, we do the feature selection first. We maintain all the features used in the Gb-S and select another 300 features (neural nodes): (i) We use all the features to train a Lasso model and select 100 neural nodes with the highest absolute coefficient values; (ii) By calculating the mutual information between any neural node and the label (correct or not), we select another 100 features possessing top absolute mutual information; (iii) We select another 100 features with top absolute Pearson correlation coefficient. After the feature selection, we train a random forest model to predict whether the response is correct based on the selected features.

In the experiment section of the main text, the features in the Wb-S for natural language generation tasks include (i) all the features used in the Gb-S, (ii) the hidden activations of the last token of the question from the middle layer (LLaMA2-7B or LLaMA3-8B: 16th layer; Gemma-7B: 14th layer), and (iii) the hidden activations of the last token of the answer from the middle layer. Therefore, in these natural language generation tasks, the dimension is 8212 for LLaMA2-7B/LLaMA3-8B and 6164 for Gemma-7B.

The features in the Wb-S for the multiple-choice task include (i) all the features used in the Gb-S and (ii) the hidden activations of the last token of the answer (letter A, B, C, or D) from the middle layer. The dimension is 4101 for LLaMA2-7B/LLaMA3-8B and 3077 for Gemma-7B.

Notably, there are many choices of the hidden activations employed in the Wb-S. Besides what has been shown in Section A, we provide further discussion in Section D.

**Bb-S.** The idea of building a supervised calibration model for a black-box LLM is to use the hidden layers and output distributions from another open-source LLM model by feeding it with the question and the provided response. Therefore, the features available for the Wb-S are also available for the open-source LLM, so we just take the corresponding features from the open-source LLM in the Bb-S. Hence, in the natural language generation tasks, the input dimension of the calibration model is 4196 (including hidden activations of the question and answer and 20 entropy and likelihood-related features,  $2 \times 2048 + 20$ ) for Gemma-2B, 6164 for Gemma-7B, 8212 for LLaMA2-7B/LLaMA3-8B, and 10260 for LLaMA2-13B. In the multiple-choice task, the dimension is 2053 for Gemma-2B (including the hidden activations of the answer and 5 entropy- and probability-related features used in the Gb-S), 3077 for Gemma-7B, 4101 for LLaMA2-7B/LLaMA3-8B, and 5125 for LLaMA2-13B.

For all these methods, we employ the random forest (Breiman, 2001) using the implementation from the scikit-learn package (Pedregosa et al., 2011) to estimate the uncertainty. The hyperparameters are set as [n\_estimators=150, random\_state=0, max\_depth=8, verbose=2, max\_features=45] if the number of selected features is no less than 100 and [n\_estimators=100, random\_state=0, max\_depth=4, verbose=2] otherwise.

## D Additional results and visualizations

In Section A, we show the advantage of utilizing the hidden activations of the *answer* from the middle layer of the LLM to estimate the uncertainty in Wb-S. In this section, we further discuss the impact of employing the hidden activations from the *question* in the Wb-S.

The motivation stems from the observation that within the transformer architecture, although the hidden activation of a question’s last token (referred to as the question’s activation) is forwarded to obtain the hidden activation of the answer’s last token (referred to as the answer’s activation), implying that the answer’s activation incorporates the question’s activation information, it has been discovered that concatenating the question’s activation with the answer’s activation offers additional insights into the answer’s uncertainty (Duan et al., 2024). We would like to further investigate the effectiveness of



incorporating the question’s activation along with the answer’s activation into the supervised setting.

We experiment with three feature combinations in our supervised setting: (i) Question: we use the hidden activation of the last token of the question from the middle layer, incorporated with the entropy- or probability-related features of the question (10 features in total listed in the right column of Table 5) if it is a natural language generation task, otherwise incorporated with all the features in Gb-S; (ii) Answer: we use the hidden activation of the last token of the answer from the middle layer incorporated with all the features used in Gb-S; (iii) Question-Answer: we use the last-token hidden activation of both the question and answer from the middle layer and all the features in Gb-S. We compare their performance with Gb-S in Figure 6 and present the following observations.

**Question itself cannot capture enough uncertainty information.** From Figure 6, we observe that the method Bb-S consistently outperforms Question across all these tasks. This implies that incorporating the features relating to the question only cannot provide enough information about the uncertainty of the answer. This aligns with the inferior performance of the sample-based method (Kuhn et al., 2023) we tested in the earlier sections. In these methods, the uncertainty score is used to estimate the language model’s uncertainty about the question. This result implies that uncertainty cannot be captured in the question by the language model without generating the answer.

**Question’s hidden activation cannot help to generate more uncertainty information** Again from Figure 6, by comparing the performance of Answer and Question-Answer, we find that the inclusion of question’s activation has little impact on improving the performance. This shows that the uncertainty from the question might have already been well encoded in the last token activation of the answer.

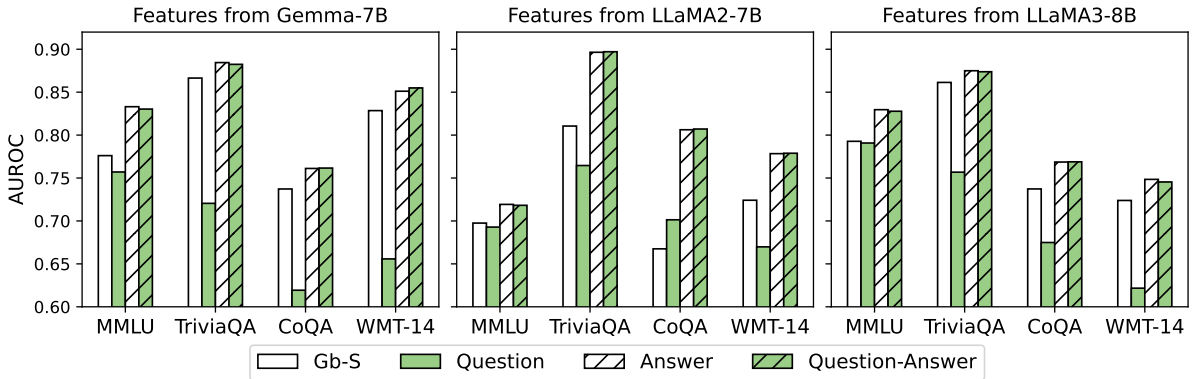


Figure 6: Performance comparison of using last-token middle layer hidden activations of the answer (Answer) or the concatenation of the question and answer (Question-Answer) as features in the Wb-S, where the features in Gb-S are also included in Wb-S. In the natural language generation tasks, the dimensions of Gb-S, Question, Answer, and Question-Answer for Gemma-7B are 20, 3082, 3092, and 6164, while for LLaMA2-7B or LLaMA3-8B they are 20, 4106, 4116, and 8212, respectively. In the MMLU task, for Gemma-7B they are 5, 3077, 3077, and 6149, while for LLaMA2-7B or LLaMA3-8B, they are 5, 4101, 4101, and 8197, respectively.

**The middle layer is still better than the last layer.** In Section A, Figure 1 shows that when using the hidden activation of the answer in the Wb-S, the middle layer of the LLM is a better choice than the last layer. The next question is: Does this conclusion still hold for using the concatenated hidden activations of the question and answer? We depict the experiment result in Figure 7, which is consistent with the conclusion drawn from Figure 1.

**Our method better characterizes the uncertainty.** We find that the grey-box and white-box features enhance the ability to characterize the dataset so that the distribution of the generated output’s uncertainty score is better correlated with the output’s correctness. According to Figure 8, we observe that with black-box features, the distributions of the uncertainty score for true and false answers are not

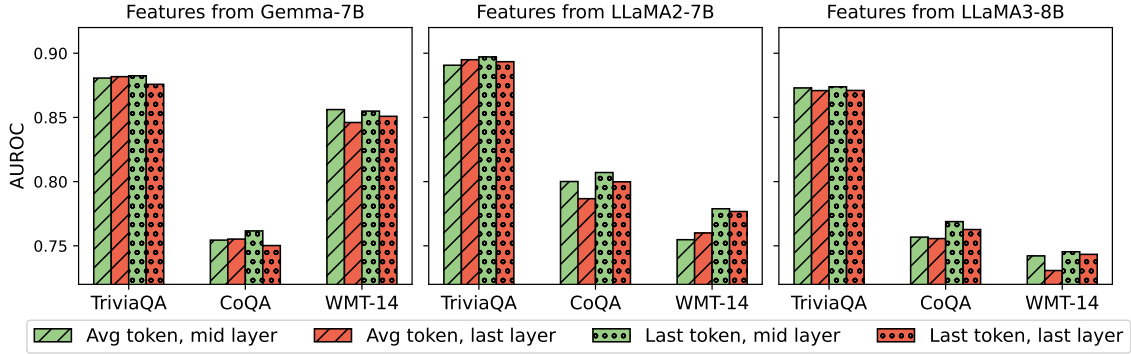


Figure 7: Performance comparison of using *question-answer concatenated* hidden activations from different tokens and layers as features in the Wb-S method. Scores are normalized in  $[0,1]$ , where a lower value indicates larger uncertainty. For Gemma-7B, the dimension of the Wb-S input is 6164 (3072 from the question, 3072 from the answer, and 20 from the grey-box features). For LLaMA2-7B/LLaMA3-8B, it is 8212.

very distinguishable, and the true answer’s distribution is even similar to a uniform distribution. With grey-box and white-box features, the distributions of the uncertainty scores are more separated between the true and false answers. The results show the supervised learning approach not only achieves better AUROC but also learns to better separate the distribution of the uncertainty scores.

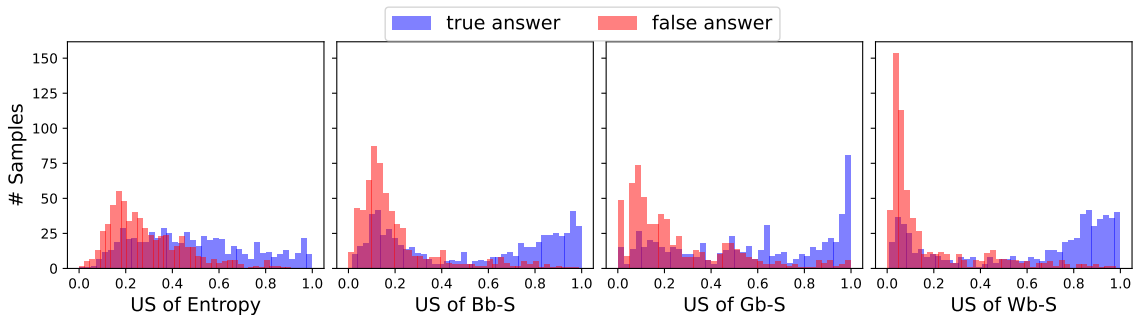


Figure 8: Uncertainty scores of different methods on the MMLU dataset for answers provided by the Gemma-7B model, where scores are normalized in  $[0,1]$ , and US is short for uncertainty score. False answer refers to the sample where the choice assigned with maximum probability by the LLM is false, while true answer represents the sample answered correctly.

## E Examples

In this section, we show some examples of the wrong answers the LLM generated and explore how different methods understand the LLM’s uncertainty. The wrong answers are selected from those samples where the LLM makes wrong predictions.

Since we let the LLM output the greedy answer, which could be wrong, we expect an ideal uncertainty estimation model to output a high confidence score when the LLM generates the correct answer, and give a low confidence score when the LLM outputs the wrong answer. By looking at different wrong answers generated by the LLM, we note that although our approach sometimes gives a high confidence score on a wrong answer generated by the LLM, at other times it shows desirable properties such as giving higher uncertainty scores to better answers, and giving low confidence score when LLM does not know the answer.

Our illustrative examples are generated as follows: For questions where the LLM’s greedy response is

incorrect, we also extract the correct answer from the dataset and additional answers randomly generated by the LLM with lower probabilities than the greedy answer. Along with these answers, we also compute the answers' corresponding metrics and features so that we can observe how they behave with different outputs. We conduct this experiment in the test dataset of TriviaQA, in which both the question and answer are short. We summarize the ways that our uncertainty estimation model behaves as follows:

- **Confidently support a wrong answer.** The LLMs are confident that the wrong greedy answer is true and assign a high confidence score. Moreover, the LLMs give low uncertainty scores to the correct answers, suggesting a lack of knowledge about these questions. We give an example of LLaMA2-7B and Gemma-7B in Figure 9 and 10. Note that in both examples, our method assigns a low uncertainty score to the correct answer and a much higher uncertainty score to the wrong answer. In contrast, the unsupervised grey-box methods assign higher uncertainty scores to the correct answer.
- **Confidently reject a wrong answer.** We give examples from LLaMA2-7B and Gemma-7B in Figure 11 and 12. The uncertainty estimation model gives a higher score to the true answer or answers that are better than the wrong answer. This means that for these questions, our model actually knows which answer is better and can assign uncertainty scores accordingly. In contrast, the unsupervised methods tend to assign much higher uncertainty scores to the greedy (wrong) answer.
- **Unconfident about any answer.** Due to the lack of knowledge, the LLM may not know the true answer. We show the examples in Figure 13 and 14. From these examples, we can see that the model assigns almost the same uncertainty scores to these generated answers, including the true answer. In this scenario, the uncertainty estimation model is uncertain about the correctness of any answer. Furthermore, it is interesting to note that the unsupervised methods exhibit similar behavior, assigning almost similar scores to other answers as well, albeit with much higher uncertainty scores. This differs from the previous two cases, where the unsupervised method behaved differently from our uncertainty estimation model.

### An example of a confidently wrong answer (LM: LLaMA2-7B)

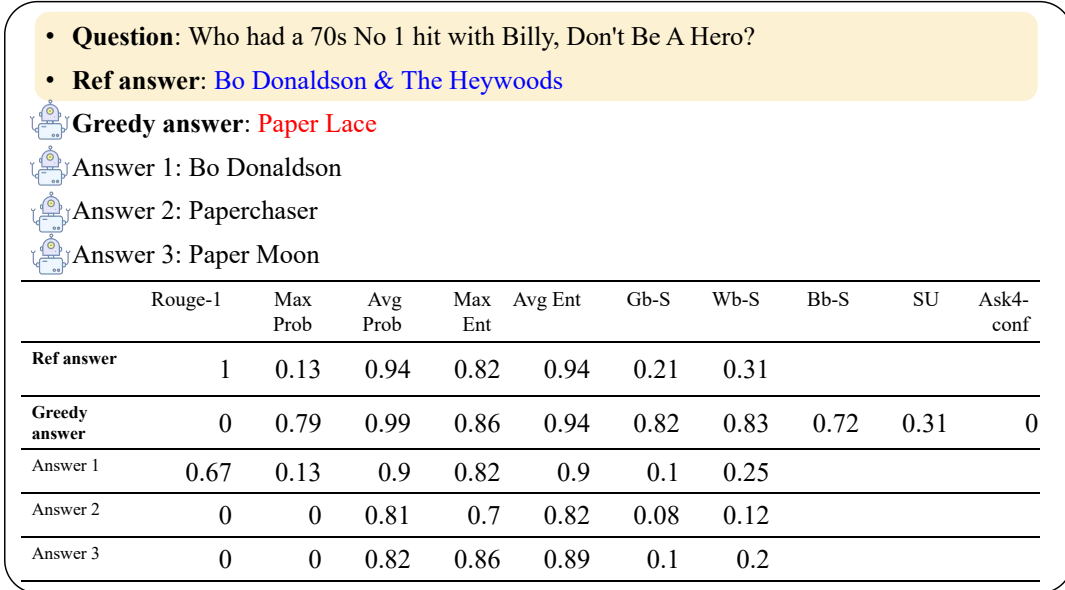


Figure 9: An example of LLaMA2-7B assigning a confidently wrong answer in the TriviaQA dataset. Scores are normalized in [0, 1], where a lower value indicates a larger uncertainty. The score of the greedy answer provided by any uncertainty estimation method is higher than that of the true answer, but the greedy answer is incorrect. The UK band Paper Lace did indeed release a version of “Billy, Don’t Be A Hero” in 1974, the same year as the version of Bo, but it was Bo Donaldson & The Heywoods (a band in the U.S.) whose version topped the charts as a No.1 hit.

### An example of a confidently wrong answer (LM: Gemma-7B)

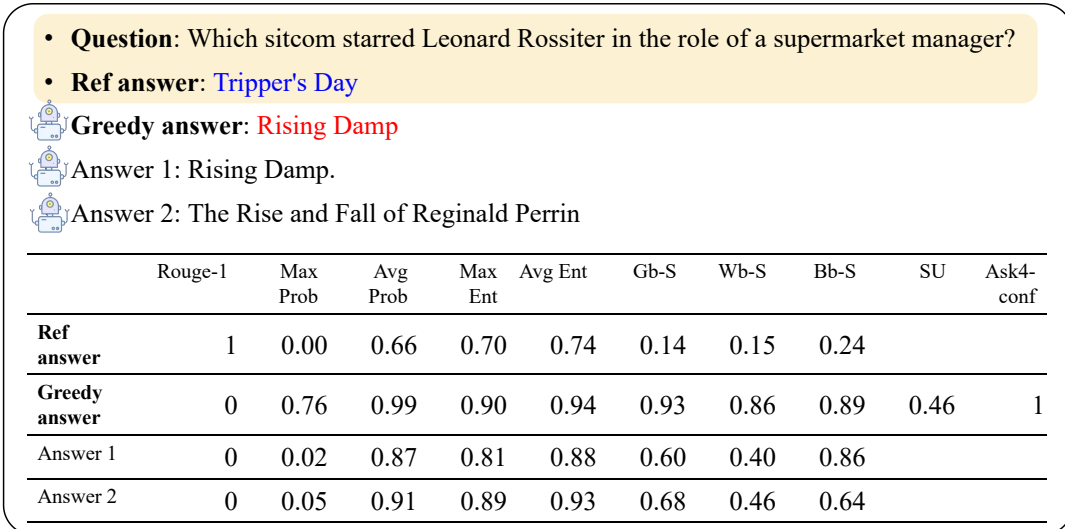


Figure 10: An example for Gemma-7B that assigns a high confidence score to a wrong answer. Leonard Rossiter starred in “Rising Damp” as a landlord, not as a supermarket manager.

### An example that the LM identifies the better answer (LM: LLaMA2-7B)

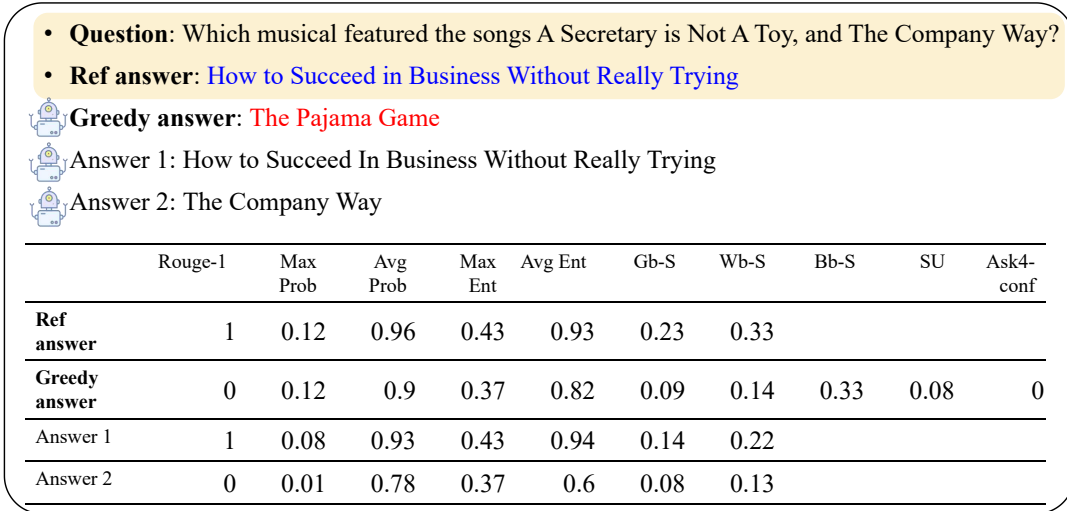


Figure 11: An example that LLaMA2-7B can successfully identify the better answer (by attaching a higher score). Scores are normalized in  $[0,1]$ , where a lower value indicates larger uncertainty.

### An example that the LM identifies the better answer (LM: Gemma-7B)

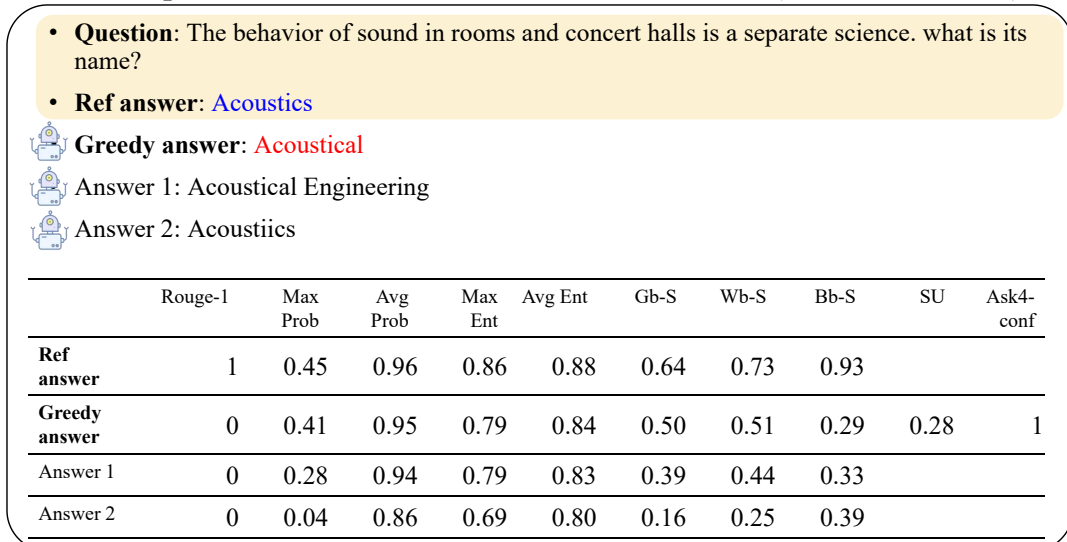





Figure 12: An example that Gemma-7B can successfully identify the better answer (by attaching a higher score). Scores are normalized in  $[0,1]$ , where a lower value indicates larger uncertainty.

An example that the LM does not know the answer (LM: LLaMA2-7B)

- **Question:** Who played Sandy Richardson in the British tv series ‘Crossroads’?
- **Ref answer:** Roger Tonge

 **Greedy answer:** Noel Clarke

 Answer 1: Mike Pratt


 Answer 2: Lucy Carless


	Rouge-1	Max Prob	Avg Prob	Max Ent	Avg Ent	Gb-S	Wb-S	Bb-S	SU	Ask4-conf
<b>Ref answer</b>	1	0.01	0.78	0.28	0.71	0.08	0.09			
<b>Greedy answer</b>	0	0.16	0.89	0.28	0.75	0.08	0.09	0.23	0	0
Answer 1	0	0.01	0.82	0.28	0.73	0.08	0.09			
Answer 2	0	0	0.71	0.28	0.63	0.08	0.08			


Figure 13: An example that LLaMA2-7B does not know the true answer. Scores are normalized in [0,1], where a lower value indicates larger uncertainty. The LM does not know the true answer and attempts to guess it by generating different names with low confidence scores, but the score is also low even when the LM faces the true answer.

An example of the failure in estimating the uncertainty (LM: Gemma-7B)

- **Question:** What is the name of the colliery in the 1939 film ‘The Stars Look Down’?
- **Ref answer:** Neptune Colliery

 **Greedy answer:** The Black Diamond

 Answer 1: Oakwood Colliery

 Answer 2: Northmoor Colliery

	Rouge-1	Max Prob	Avg Prob	Max Ent	Avg Ent	Gb-S	Wb-S	Bb-S	SU	Ask4-conf
<b>Ref answer</b>	1	0	0.62	0.19	0.65	0.10	0.13	0.23		
<b>Greedy answer</b>	0	0.02	0.72	0.18	0.20	0.10	0.10	0.12	0	1
Answer 1	0	0	0.73	0.18	0.57	0.10	0.11	0.18		
Answer 2	0	0	0.73	0.18	0.53	0.10	0.12	0.19		

Figure 14: An example that Gemma-7B does not know the true answer. Scores are normalized in [0,1], where a lower value indicates larger uncertainty.